

See discussions, stats, and author profiles for this publication at: <https://www.researchgate.net/publication/327602171>

# The surface-atmosphere exchange of carbon dioxide in tropical rainforests: Sensitivity to environmental drivers and flux measurement methodology

Article in *Agricultural and Forest Meteorology* · September 2018

DOI: 10.1016/j.agrformet.2018.09.001

CITATIONS

0

READS

923

22 authors, including:



**Zheng Fu**

Chinese Academy of Sciences

9 PUBLICATIONS 41 CITATIONS

[SEE PROFILE](#)



**Tobias Gerken**

Pennsylvania State University

49 PUBLICATIONS 295 CITATIONS

[SEE PROFILE](#)



**Gabriel Bromley**

Montana State University

5 PUBLICATIONS 4 CITATIONS

[SEE PROFILE](#)



**Alessandro Carioca de Araújo**

Brazilian Agricultural Research Corporation (EMBRAPA)

109 PUBLICATIONS 2,764 CITATIONS

[SEE PROFILE](#)

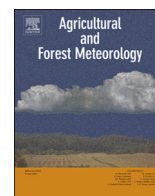
Some of the authors of this publication are also working on these related projects:



CRESCENDO H2020 [View project](#)



Create new project "LBA-EUSTACH" [View project](#)



## The surface-atmosphere exchange of carbon dioxide in tropical rainforests: Sensitivity to environmental drivers and flux measurement methodology



Zheng Fu<sup>a,b,c</sup>, Tobias Gerken<sup>a</sup>, Gabriel Bromley<sup>a</sup>, Alessandro Araújo<sup>d</sup>, Damien Bonal<sup>e</sup>, Benoît Burban<sup>f</sup>, Darren Ficklin<sup>g</sup>, Jose D. Fuentes<sup>h</sup>, Michael Goulden<sup>i</sup>, Takashi Hirano<sup>j</sup>, Yoshiko Kosugi<sup>k</sup>, Michael Liddell<sup>l,m</sup>, Giacomo Nicolini<sup>n,o</sup>, Shuli Niu<sup>b</sup>, Olivier Roupsard<sup>p,q</sup>, Paolo Stefani<sup>n</sup>, Chunrong Mi<sup>r</sup>, Zaddy Tofte<sup>a</sup>, Jingfeng Xiao<sup>s</sup>, Riccardo Valentini<sup>n,o</sup>, Sebastian Wolf<sup>t</sup>, Paul C. Stoy<sup>a,\*</sup>

<sup>a</sup> Department of Land Resources and Environmental Sciences, Montana State University, Bozeman, MT 59717, USA

<sup>b</sup> Key Laboratory of Ecosystem Network Observation and Modeling, Institute of Geographic Sciences and Natural Resources Research, Chinese Academy of Sciences, Beijing 100101, China

<sup>c</sup> University of Chinese Academy of Sciences, No.19A Yuquan Road, Beijing 100049, China

<sup>d</sup> Embrapa Amazônia Oriental, Belém, PA, Brazil

<sup>e</sup> Université de Lorraine, AgroParisTech, INRA, UMR Silva, 54000 Nancy, France

<sup>f</sup> INRA, UMR Ecofog, 97310 Kourou, French Guiana

<sup>g</sup> Department of Geography, Indiana University, 701 Kirkwood Ave., Bloomington, Indiana 47405, USA

<sup>h</sup> Department of Meteorology and Atmospheric Science, The Pennsylvania State University, University Park, PA, USA

<sup>i</sup> Department of Earth System Science, University of California, Irvine, CA 92697, USA

<sup>j</sup> Research Faculty of Agriculture, Hokkaido University, Sapporo, Japan

<sup>k</sup> Laboratory of Forest Hydrology, Graduate School of Agriculture, Kyoto University, 606-8502 Japan

<sup>l</sup> Centre for Tropical, Environmental, and Sustainability Sciences, College of Science and Engineering, James Cook University, P.O. Box 6811, Cairns, Queensland 4870, Australia

<sup>m</sup> Terrestrial Ecosystem Research Network, Australian SuperSite Network, James Cook University, P.O. Box 6811, Cairns, Queensland 4870, Australia

<sup>n</sup> University of Tuscia, DIBAF Department, Via San Camillo de Lellis, 01100 Viterbo, Italy

<sup>o</sup> Euro-Mediterranean Center on Climate Change (CMCC), IAFES Division. Viale Trieste 127, 01100 Viterbo, Italy

<sup>p</sup> CIRAD, UMR Eco&Sols, 2 Place Viala, 34060 Montpellier, France

<sup>q</sup> CATIE, Centro Agronómico Tropical de Investigación y Enseñanza, Turrialba, Costa Rica

<sup>r</sup> Key Laboratory of Water Cycle and Related Land Surface Processes, Institute of Geographic Sciences and Natural Resources Research, University of Chinese Academy of Sciences, Beijing 100101, China

<sup>s</sup> Earth Systems Research Center, Institute for the Study of Earth, Oceans, and Space, University of New Hampshire, Durham, NH 03824, USA

<sup>t</sup> Department of Environmental Systems Science, ETH Zurich, 8092 Zurich, Switzerland

### ARTICLE INFO

#### Keywords:

Climate variability  
Ecosystem respiration  
Eddy covariance  
Gross primary productivity  
Net ecosystem carbon dioxide exchange  
Tropical rainforest

### ABSTRACT

Tropical rainforests play a central role in the Earth system by regulating climate, maintaining biodiversity, and sequestering carbon. They are under threat by direct anthropogenic impacts like deforestation and the indirect anthropogenic impacts of climate change. A synthesis of the factors that determine the net ecosystem exchange of carbon dioxide (NEE) at the site scale across different forests in the tropical rainforest biome has not been undertaken to date. Here, we study NEE and its components, gross ecosystem productivity (GEP) and ecosystem respiration (RE), across thirteen natural and managed forests within the tropical rainforest biome with 63 total site-years of eddy covariance data. Our results reveal that the five ecosystems with the largest annual gross carbon uptake by photosynthesis (i.e.  $GEP > 3000 \text{ g C m}^{-2} \text{ y}^{-1}$ ) have the lowest net carbon uptake – or even carbon losses – versus other study ecosystems because RE is of a similar magnitude. Sites that provided sub-canopy  $\text{CO}_2$  storage observations had higher average magnitudes of GEP and RE and lower average magnitudes of NEE, highlighting the importance of measurement methodology for understanding carbon dynamics in ecosystems with characteristically tall and dense vegetation. A path analysis revealed that vapor pressure deficit (VPD) played a greater role than soil moisture or air temperature in constraining GEP under light saturated conditions across most study sites, but to differing degrees from  $-0.31$  to  $-0.87 \mu\text{mol CO}_2 \text{ m}^{-2} \text{ s}^{-1} \text{ hPa}^{-1}$ . Climate projections from 13 general circulation models (CMIP5) under the representative concentration pathway that

\* Corresponding author.

E-mail address: [paul.stoy@montana.edu](mailto:paul.stoy@montana.edu) (P.C. Stoy).

<https://doi.org/10.1016/j.agrformet.2018.09.001>

Received 21 December 2017; Received in revised form 8 August 2018; Accepted 1 September 2018

0168-1923/ © 2018 Elsevier B.V. All rights reserved.

generates  $8.5 \text{ W m}^{-2}$  of radiative forcing suggest that many current tropical rainforest sites on the lower end of the current temperature range are likely to reach a climate space similar to present-day warmer sites by the year 2050, warmer sites will reach a climate not currently experienced, and all forests are likely to experience higher VPD. Results demonstrate the need to quantify if and how mature tropical trees acclimate to heat and water stress, and to further develop flux-partitioning and gap-filling algorithms for defensible estimates of carbon exchange in tropical rainforests.

## 1. Introduction

Tropical rainforests regulate the amount of heat and moisture that enters the atmosphere in the tropics (Avissar and Werth, 2005), act as a critical reservoir for biodiversity (Gibson et al., 2011), and serve as a globally important stock of carbon (Dixon et al., 1994; Phillips et al., 1998). They may be turning into a net source of carbon to the atmosphere due largely to degradation and disturbance (Baccini et al., 2017). Such threats to tropical rainforests affect not only their carbon dynamics, but also the other ecosystem and Earth system services that rainforests provide (Foley et al., 2005; Kim et al., 2015; Mitchard, 2018), and emphasize the need to understand the functional diversity of rainforests for a deeper understanding of the Earth system (Asner et al., 2017; Levine et al., 2016; Pavlick et al., 2013).

Inverse and forward modeling approaches demonstrate that tropical forests contribute  $\sim 20\%$  of the interannual variability of global net biome production (net carbon flux including fire emissions) (Ahlström et al., 2015), but up to  $1/3$  of the interannual variability of biosphere-atmosphere carbon dioxide ( $\text{CO}_2$ ) flux in the southern hemisphere (Fu et al., 2017). Satellite observations demonstrate diverse patterns of carbon fluxes within the tropical rainforest biome; for example, the standard deviation of gross ecosystem productivity (GEP) estimated from Moderate Resolution Imaging Spectroradiometer (MODIS) is higher across some tropical rainforest areas - especially in southeast Asia, coastal Africa, and the western Amazon - than many other global ecosystems (Fig. 1, Xiao et al., (2016)). Such observations motivate the

need to study the controls over carbon fluxes in the natural and increasingly managed ecosystems of the tropical rainforest biome (Hall et al., 1995).

Much has been learned about the net surface-atmosphere exchange (NEE) of  $\text{CO}_2$  since the first eddy covariance measurements of *terra firme* tropical rainforests demonstrated a substantial carbon sink on daily timescales (Grace et al., 1996, 1995; Malhi et al., 1998; Oberbauer et al., 2000). Tropical rainforests tend to have lower carbon use efficiency than temperate forests (Chambers et al., 2004), emphasizing the critical role of ecosystem respiration (RE) to the tropical carbon balance. Counterintuitive seasonal  $\text{CO}_2$  flux patterns are now resolved; tropical rainforest GEP is often greater in the dry season due to leaf emergence (Aguilos et al., 2018; Huete et al., 2008, 2006; Hutrya et al., 2007; Lopes et al., 2016; Saleska et al., 2016, 2007, 2003) despite strong limitations to GEP when water is limiting (Kiew et al., 2018; Wu et al., 2017) and a “brown down” due to water limitation toward drier regions (Saleska et al., 2009). Some studies find that tropical rainforest trees tend to be isohydric (Fisher et al., 2006; Konings and Gentine, 2016), suggesting that they tightly regulate stomatal conductance under conditions of water stress including when the vapor pressure deficit (VPD) is high. However, tropical trees exhibit a range of hydraulic behavior (Braga et al., 2016; Giardina et al., 2018; Klein, 2014; Powell et al., 2017; Siddiq et al., 2017) and modeling studies suggest that anisohydric strategies may be preferred in tropical systems with little risk of water stress (Inoue et al., 2016; Kumagai and Porporato, 2012). These climate and hydrologic stresses are coupled with

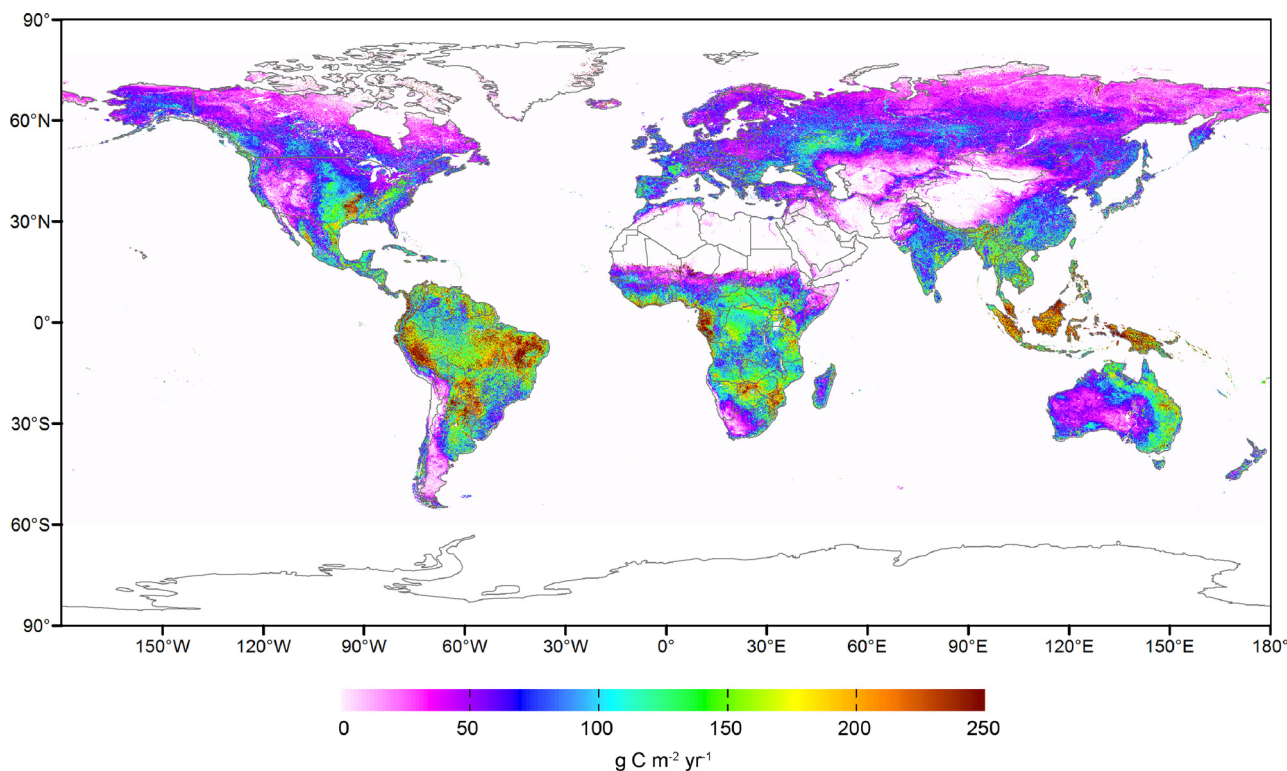


Fig. 1. The standard deviation of annual gross ecosystem productivity (GEP) from MODIS (MOD17A3) for the period.2000–2015. (For interpretation of the references to color in the figure the reader is referred to the web version of this article.)

management pressures that impact carbon fluxes in tropical ecosystems.

Forests in the tropical rainforest biome are increasingly managed, and managed ecosystems must also be studied for a comprehensive understanding of carbon metabolism in the tropics. Reforestation tends to increase carbon sequestration (Wolf et al., 2011b, 2011c), but responses of tropical rainforests to other anthropogenic and natural disturbances, such as deforestation (Pan et al., 2011), fire (van Marle et al., 2017) and drought (Bonal et al., 2008; Phillips et al., 2009) are diverse and interactive. For example, a tropical peat forest near Palangkaraya, Indonesian Borneo (ID-Pag; see Table 1) was a net source of CO<sub>2</sub> to the atmosphere over multiple years due to constraints on GEP by VPD, radiative perturbations due to peat fire smoke, and perturbation of the water table (Hirano et al., 2012; 2008; 2007). These and other factors create large interannual variability in tropical rainforest NEE (e.g. Fig. 1) that remains poorly understood at the ecosystem scale.

Studying the annual and interannual variability in tropical rainforest carbon exchange at the ecosystem scale is challenging due to the unique difficulties that they present to the eddy covariance methodology (Kruijt et al., 2004; Miller et al., 2004). Intact tropical forests tend to be at remote sites away from line power sources, which creates logistical challenges for making quasi-continuous long-term measurements. Tropical rainforest canopies are characteristically tall and dense, resulting in complex within-canopy atmospheric transport (Fuentes et al., 2016; Gerken et al., 2017; Tóta et al., 2012) that makes standard approaches for measuring and modeling nighttime ecosystem respiration difficult to apply (Dargie et al., 2017; de Araújo et al., 2010; Grace et al., 2016; Loeschner et al., 2003; Pan et al., 2011; Santos et al., 2016). Alternate approaches for estimating nighttime RE based on daytime flux measurements (e.g. Lasslop et al., (2010)) may represent an improvement, but the sensitivity of tropical rainforest carbon fluxes to flux partitioning methods across different ecosystems has not been studied to date.

Despite these and other challenges, there is a pressing need to quantify surface-atmosphere carbon exchange across managed and (quasi-) unmanaged ecosystems in the tropical rainforest biome to further understand their role in the Earth system. As a critical step in this process, the impacts of methodological approaches and environmental drivers on carbon exchange need to be investigated. Here, we study NEE and its components, GEP and RE, across thirteen natural and managed tropical forest ecosystems in seven countries in all five continents where tropical rainforests exist. We place particular emphasis on the relationship between surface-atmosphere carbon exchange and environmental drivers and critique different eddy covariance data processing approaches with an eye toward methodological improvements. The goal of this paper is to synthesize observations of NEE and its components in managed and unmanaged tropical rainforests and to highlight important current and future directions for studying tropical rainforest carbon metabolism in a changing climate.

## 2. Materials and methods

### 2.1. Study sites

For the purposes of this study we define tropical rainforests as comprising characteristic evergreen broadleaf vegetation (Fig. 2) rather than inhabiting a climate zone with the absence of a dry season, given that severe droughts can and do occur in tropical rainforests (Lewis et al., 2011). We also include managed ecosystems given their increasing importance to the carbon cycle of the tropical rainforest biome (Tyukavina et al., 2015). By this definition we include the site BR-Ban (Table 1) on the tropical rainforest – cerrado ecotone (Borma et al., 2009; da Rocha et al., 2009) as well as reforested (PA-SPn) and managed (VU-Coc) tropical rainforests (Table 1). We exclude sites with characteristic savanna, subtropical, or tropical dry forest vegetation, noting some subjectivity in the definition of what constitutes a tropical

**Table 1** Tropical rainforest eddy covariance sites explored in the present study. Observations come from both the LaThuille and FLUXNET2015 databases. Sites indicated by + were available only for the LaThuille database. # indicates managed ecosystems. ‘System’ indicates the use of open (OP) or closed path (CP) eddy covariance systems. ‘Unk’ indicates unknown.

Site ID	Lat.	Long.	Observation period	Forest age (year)	Canopy height (m)	Leaf area index (m <sup>2</sup> m <sup>-2</sup> )	Soil depth (m)	Water table depth (m)	Carbon storage	System	Gap-filling (%)	References
AU-Rob	-17.1175	145.6301	2014-2014	Unk	28	3.2	> 8	~ 6	No	OP	61%	(Beringer et al., 2016; Bradford et al., 2014)
BR-Ban <sup>+</sup>	-9.8244	-50.1591	2003-2006	Unk	18	3.5-4.5	3	3.7-4.5	No	OP	46%	(Borma et al., 2009; da Rocha et al., 2009; Restrepo-Coupe et al., 2013)
BR-Cax <sup>+</sup>	-1.7197	-51.4590	1999-2003	Unk	30-35	5.1	3-4	~ 10 (wet season)	No	CP	79%	(Carswell et al., 2002; Restrepo-Coupe et al., 2013)
BR-Ji2 <sup>+</sup>	-10.0832	-61.9309	2000-2002	Unk	30	5.5	1.2-4	Unk	No	CP	36%	(Andraee et al., 2002; Kruijt et al., 2004; Meir et al., 2001)
BR-Ma2 <sup>+</sup>	-2.6091	-60.2093	1999-2006	Unk	30-35	4.7	> 15	35	No	CP	45%	(Araújo et al., 2002; Restrepo-Coupe et al., 2013)
BR-Sa1	-2.8567	-54.9589	2002-2011	Unk	35-40	6.0	> 12	> 100	Yes	CP	63%	(Martens et al., 2004; Nepstad et al., 2002; Restrepo-Coupe et al., 2013)
BR-Sa3	-3.0180	-54.9714	2000-2004	> 100	35-40	4.9	> 12	> 100	Yes	CP	62%	(Goulden et al., 2006; Restrepo-Coupe et al., 2013)
GF-Guy	5.2777	-52.9288	2004-2014	Unk	35-40	7.0	> 5	1-30	Yes	OP	55%	(Bonal et al., 2008)
GH-Ank	5.2685	-2.6942	2011-2014	Unk	25-30	5.9	≥ 1	≥ 1	Yes	CP	72%	(Belleli Marchesini et al., 2008; Chiti et al., 2010)
ID-Pag <sup>+</sup>	-2.3450	114.0360	2002-2003	> 50	26	5.6	4 (Peat depth)	0.2-1.7	Yes	OP	65%	(Hirano et al., 2007)
MY-PSO	2.9730	102.3062	2003-2009	Unk	35	6.5	Unk	Unk	Yes	OP	69%	(Kosugi et al., 2008, 2012)
PA-SPn <sup>#</sup>	9.3181	-79.6346	2007-2009	6-8	8-12	3.0-5.4	> 1	Unk	Yes	OP	75%	(Wolf et al., 2011a,b,c)
VU-Coc <sup>+, #</sup>	-15.4427	167.1920	2001-2004	> 20	16	5.6	Unk	Unk	No	OP	47%	(Navarro et al., 2008; Rouspard et al., 2006)

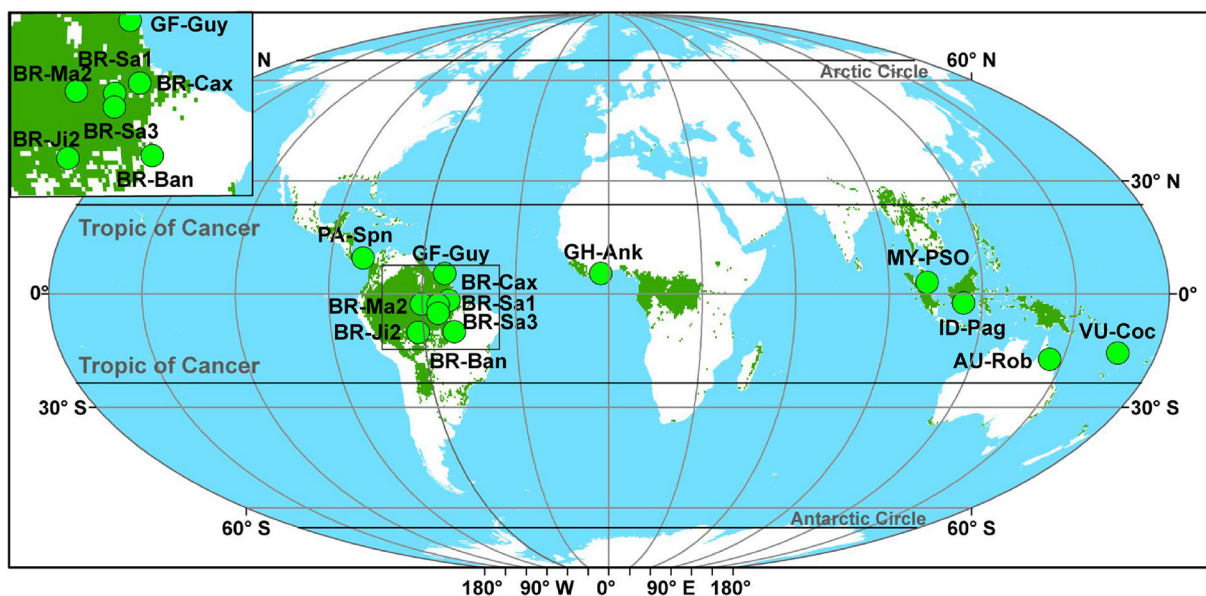


Fig. 2. A map of global tropical rainforest area (in green) based on the MODI MCD12C1 land cover classification with the location and distribution of the 13 tropical rainforest eddy covariance sites used in this study (see Table 1).

rainforest. We analyze surface-atmosphere exchange observations obtained from the LaThuille and FLUXNET2015 databases for 13 tropical rainforests located in Australia, Brazil, French Guiana, Ghana, Malaysia, Panama, and Vanuatu (Fig. 2) and summarize key variables in Table 1, which also lists respective publications in which additional site information is available. We use the conventions that GEP and RE are positive quantities and that  $NEE = RE - GEP$  such that net C uptake by the biosphere is denoted as negative per the atmospheric convention.

## 2.2. The LaThuille and FLUXNET2015 databases

We explored data from both the LaThuille and FLUXNET2015 databases. Both databases harmonize, standardize, and gap-fill half-hourly or hourly observations of NEE submitted by Principal Investigators from regional flux networks. The LaThuille database standardizes flux observations following Papale et al., (2006) and Reichstein et al., (2005), and uses nighttime RE observations under conditions of sufficient friction velocity ( $u_*$ ) to model RE during daytime and thus estimate GEP by the difference between modeled RE and measured NEE. The FLUXNET2015 database uses additional daytime flux partitioning approaches (Lasslop et al., 2010) to estimate GEP and RE, and includes multiple uncertainty estimates about each approach. For sites included in both databases, we focus on the longer FLUXNET2015 records and compare flux estimates from both databases for completeness. We note that subcanopy  $CO_2$  storage is required for the calculation of NEE in the FLUXNET2015 dataset but not the LaThuille dataset, and that carbon flux estimates from FLUXNET processing algorithms may differ from those determined by Principal Investigators. Additional information with regards to flux processing in the FLUXNET2015 dataset is provided in Appendix A.

## 2.3. Data analysis

We analyze the sensitivity of NEE, GEP, and RE to flux methodology amongst the 13 study sites and characterize differences in the response of tropical canopies to atmospheric water stress via the VPD (Kiew et al., 2018; Wu et al., 2017) given the intermittent availability of soil moisture measurements and to account for recent arguments that VPD will increasingly constrain canopy conductance and thereby GEP

(Novick et al., 2016; Sulman et al., 2016). We critique the notion that VPD is responsible for the decline in light-saturated GEP and NEE using a path analysis that also includes soil water content (SWC) and air temperature ( $T_a$ ) and their interactions to account for soil hydraulic limitations to productivity and the role of high temperatures in enzyme denaturation. We first designed the path diagrams for their correlations as in Fig. A1;  $T_a$ , VPD and SWC affect GEP or NEE under light-saturated conditions, and all micrometeorological variables are directly related (as is the case with  $T_a$  and VPD) or correlated. To derive the final path diagram, we ran the path analysis multiple times, removing insignificant paths with P-values  $> 0.05$  on each iteration, until all remaining paths were statistically significant. The path value (PV, arrow thickness in Fig. A1) was derived from the standardized partial regression coefficients, representing the relative strength of a given relationship. The PV was designed to quantitatively compare the relative influence of  $T_a$ , VPD and SWC on GEP and NEE under light-saturated conditions. The path model was fitted using the ‘lavaan’ package in R3.0.2 for Mac and we use the convention that carbon uptake by the biosphere is denoted as positive (i.e.  $-NEE$ ) in the path analysis to use the same sign convention as GEP to simplify comparison.

## 2.4. General circulation models

To ascertain the projected climate state of the study sites, monthly averages of  $T_a$  and VPD from 13 General Circulation Models (GCMs) were obtained from the Coupled Model Intercomparison Project - Phase 5 archive (CMIP5, Table A2) (Taylor et al., 2012) for Representative Concentration Pathway 8.5 (high emissions scenario). These models were previously downscaled to  $0.5^\circ$  grid using the Bias Correction – Spatial Downscaling method (Wood et al., 2004). Thirteen different models comprised the ensemble and were averaged together to create a single monthly time series for the model grid cells that contain the sites for each variable from 1950 to 2050. Annual averages and standard deviations were calculated from the monthly means. Atmospheric vapor pressure ( $e_a$ ) was estimated by assuming that when  $T_a$  is close to its daily minimum it is saturated with water vapor such that relative humidity is close to 100% (i.e. the dewpoint temperature was assumed to be near the daily minimum temperature) following Roderick and Farquhar (2002).

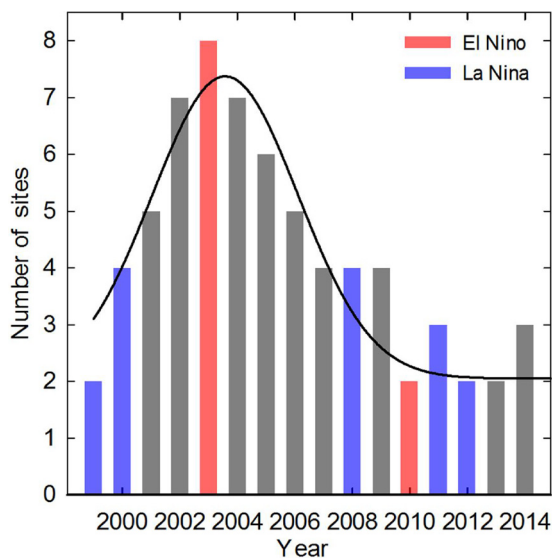


Fig. 3. The number of tropical rainforest eddy covariance research sites per year with data archived in the LaThuile and/or FLUXNET2015 databases as of March 2017.

### 3. Results

#### 3.1. Data availability

More tropical forest eddy covariance sites provided data to FLUXNET in the past, (e.g. data from eight sites from the year 2003 are available for analysis) than in more recent years; as of 2018 only two sites are available for the El Niño year of 2010 and the La Niña year of 2012 (Fig. 3). While there were more La Niña years than El Niño years

in the available period (Fig. 3), more sites were affected by the 2003 El Niño. Our results are subject to this asymmetry of data availability among years.

#### 3.2. Meteorological variability

We used daily mean meteorological data to compare mean monthly meteorological characteristics among sites. Mean  $T_a$  was approximately 26 °C at BR-Ban, BR-Cax, BR-Sa1, BR-Ma2, BR-Sa3, GF-Guy and MY-PSO and approximately 25 °C in BR-Ji2, GH-Ank, VU-Coc, and PA-SPn (Fig. 4a). AU-Rob experienced cooler conditions and was more seasonal with a mean monthly ( $\pm$  standard deviation)  $T_a$  of  $21.7 \pm 2.6$  °C, while ID-Pag was the hottest and the least seasonal with a mean monthly  $T_a$  of  $26.6 \pm 0.4$  °C (Fig. 4a). Similarly, the highest monthly soil temperature ( $T_s$ ) was found at ID-Pag ( $27.4 \pm 0.4$  °C, Fig. 4e) and the lowest at AU-Rob ( $18.9 \pm 2.6$  °C). BR-Ban had the highest monthly mean and standard deviation of VPD ( $12.2 \pm 5.6$  hPa, Fig. 4d). BR-Sa3 ( $9.0 \pm 2.2$  hPa) and ID-Pag ( $8.1 \pm 1.3$  hPa) had a larger monthly VPD than MY-PSO, BR-Ma2, GF-Guy, BR-Sa1 (all  $\sim 6.0 \pm 1.2$  hPa, Fig. 4d), while GH-Ank ( $3.0 \pm 1.4$  hPa) and AU-Rob ( $4.4 \pm 1.6$  hPa) had the lowest monthly mean VPD (Fig. 4d). Monthly mean precipitation and PPFD were both highly variable at all 13 sites, on average  $5.6 \pm 4.0$  mm/day and  $402.6 \pm 63.4$   $\mu\text{mol m}^{-2} \text{s}^{-1}$ , respectively (Fig. 4b, c). BR-Ban had the highest monthly mean PPFD ( $488.1 \pm 64.5$   $\mu\text{mol m}^{-2} \text{s}^{-1}$ ) while monthly mean PPFD at GH-Ank was the lowest amongst the 13 sites ( $297.4 \pm 65.3$   $\mu\text{mol m}^{-2} \text{s}^{-1}$ , Fig. 4c). Monthly mean soil water content in VU-Coc ( $44.7 \pm 5.8\%$ ), MY-PSO ( $41.6 \pm 2.7\%$ ), PA-SPn ( $39.1 \pm 9.9\%$ ), and BR-Cax ( $38.6 \pm 4.5\%$ ) was higher than that of GF-Guy and GH-Ank ( $18.9 \pm 3.3\%$ , Fig. 4f), noting that not all sites were able to provide VPD, PPFD,  $T_s$  and soil water content observations.

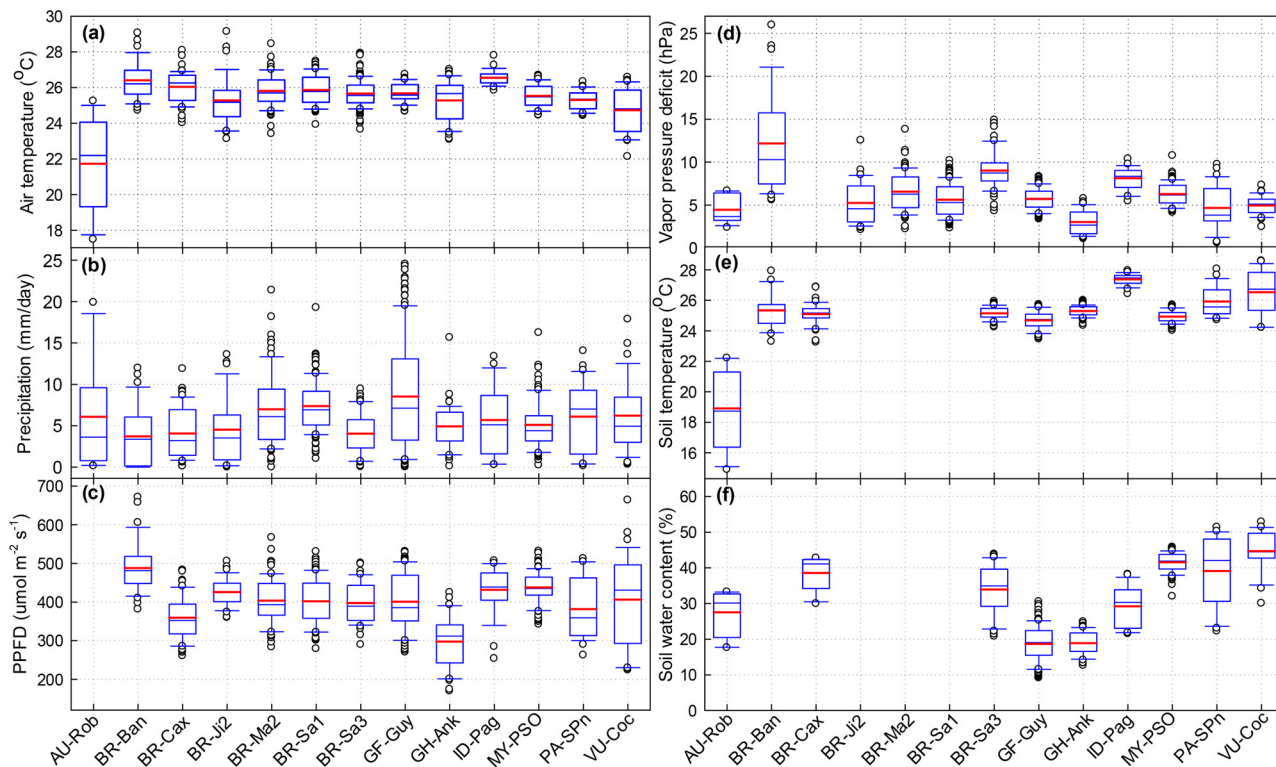


Fig. 4. Median (blue) and average (red) monthly above-canopy air temperature (a), precipitation (b), photosynthetic photon flux density (PPFD, c), vapor pressure deficit (d), soil temperature (e), and soil water content (f) from daily mean observations with boxes representing, from top to bottom, 95th, 75th, 50th, 25th, and 5th percentiles. (For interpretation of the references to colour in this figure legend, the reader is referred to the web version of this article.)

### 3.3. Carbon fluxes in tropical rainforests: trends and sensitivity to flux methodology

We compare carbon flux values obtained using nighttime partitioning methods from both the LaThuile and FLUXNET2015 databases, and then discuss differences between daytime and nighttime partitioning methods from the FLUXNET2015 database. The cumulative sum of NEE using nighttime partitioning methods (Fig. A2) exhibits differences in magnitude and sometimes sign amongst sites during the observation periods (Table 1). At ID-Pag, approximately  $700 \text{ g C m}^{-2}$  of carbon (or  $\sim 350 \text{ g C m}^{-2} \text{ y}^{-1}$ ) was released to the atmosphere over two years (Fig. A2). MY-PSO took up  $7000 \text{ g C m}^{-2}$  during the seven-year available observation period or  $\sim 1000 \text{ g C m}^{-2} \text{ y}^{-1}$  (Fig. A2a and Table 2). BR-Ban, BR-Ma2, and BR-Cax were also measured to be net carbon sinks (i.e. negative NEE) on the order of  $-1000 \text{ g C m}^{-2} \text{ y}^{-1}$ , but the carbon sinks at BR-Sa1, GF-Guy and BR-Sa3 were weaker, approximately  $-200 \text{ g C m}^{-2} \text{ y}^{-1}$  on average (Table 2, Fig. A2a).

The cumulative sum of RE (Fig. A2c) using nighttime partitioning techniques showed large differences while the cumulative sum of GEP (Fig. A2b) was less variable during the available observation periods. Mean annual RE ranged from  $1430 \text{ g C m}^{-2} \text{ y}^{-1}$  (BR-Ban) to  $3580 \text{ g C m}^{-2} \text{ y}^{-1}$  (ID-Pag) across the 13 sites while mean annual GEP ranged from  $2330 \text{ g C m}^{-2} \text{ y}^{-1}$  at PA-SPn to  $3720 \text{ g C m}^{-2} \text{ y}^{-1}$  at GF-Guy (Table 2, Fig. A2).

RE estimated from daytime partitioning approaches tended to be larger than those derived from nighttime partitioning approaches; for example, RE at BR-Sa1 estimated from daytime partitioning approaches was larger than that of nighttime partitioning approaches by  $560 \text{ g C m}^{-2} \text{ y}^{-1}$  on average ( $P < 0.05$ , Tables 2 and A3). We proceed with our analysis by comparing GEP and RE derived from nighttime partitioning approaches simply because more data are available to analyze (Table 2) while noting important differences in C flux estimates that result from differences in partitioning methodology.

An ANOVA coupled to a least-significant difference test for multiple comparisons (Rice, 1989) demonstrated that the 13 sites (using nighttime partitioning approaches) can be separated at the  $P < 0.05$  level into the five sites that represent a relatively weak mean annual C sink with a NEE less negative than  $-400 \text{ g C m}^{-2} \text{ y}^{-1}$  (GF-Guy, VU-Coc, BR-Sa3, BR-Sa1) or even a C source (ID-Pag), the four sites (BR-Ma2, MY-PSO, BR-Cax and BR-Ban) that represented a stronger C sink of less than  $-900 \text{ g C m}^{-2} \text{ y}^{-1}$ , and the remaining four sites with NEE between  $-400$

and  $-900 \text{ g C m}^{-2} \text{ y}^{-1}$  (Table 2, Fig. 5). Perhaps counter-intuitively, the sites that represented a weaker net ecosystem C uptake (i.e. those with NEE values closer to zero, Fig. A2) had higher GEP (greater than  $3000 \text{ g C m}^{-2} \text{ y}^{-1}$  for all sites) and higher RE (greater than  $3000 \text{ g C m}^{-2} \text{ y}^{-1}$  for all sites, Fig. 5). Four of these five sites with the exception of VU-Coc provided subcanopy carbon storage observations to the FLUXNET database (Table 1). In contrast, the sites that represented a stronger net ecosystem C uptake had lower GEP (less than  $2800 \text{ g C m}^{-2} \text{ y}^{-1}$  for all sites, Fig. 5b) and RE (less than  $1800 \text{ g C m}^{-2} \text{ y}^{-1}$  for all sites, Fig. 5c). Three of these four sites with the exception of MY-PSO were unable to provide subcanopy C storage observations to the FLUXNET database (Table 1).

### 3.4. Responses of tropical rainforest carbon flux to environmental variability

There was a strong relationship between half-hourly or hourly GEP and VPD during periods of high PPFD which was rather insensitive when thresholding observations to include PPFD values greater than  $1300 \mu\text{mol m}^{-2} \text{ s}^{-1}$  (Fig. 6). For a conservative interpretation of light saturated conditions, we chose PPFD values greater than  $1500 \mu\text{mol m}^{-2} \text{ s}^{-1}$  following Wu et al. (2017) to explore the relationship between VPD and GEP (Fig. 7), which demonstrates a variety of slopes ranging from  $-0.31 \mu\text{mol CO}_2 \text{ m}^{-2} \text{ s}^{-1} \text{ hPa}^{-1}$  (AU-Rob) to  $-0.87 \mu\text{mol CO}_2 \text{ m}^{-2} \text{ s}^{-1} \text{ hPa}^{-1}$  (PA-SPn).

Relationships between VPD and GEP alone are not necessarily indicative that VPD is the primary control over the decrease in GEP at high light levels because VPD is correlated with  $T_a$  and SWC, each of which exert independent controls over GEP (Fig. A1), which itself is subject to the assumptions of the partitioning routine used to estimate it from NEE observations. VPD,  $T_a$ , and SWC are related under light saturated conditions in most instances, as expected, at the seven ecosystems in which  $T_a$ , VPD and SWC observations were available (Table A4). The path analyses for GEP demonstrates that VPD ( $-0.54$ ) and SWC ( $-0.31$ ) have direct negative effects on GEP under light saturated conditions across these seven sites, but the response of  $T_a$  is on average positive ( $0.28$ , Table 3). A similar pattern holds for the constraints on NEE at high PPFD (Table 4), but the effect of VPD ( $-0.45$ ) is even stronger in relative terms than that of SWC ( $-0.08$ ) and  $T_a$  again has a positive effect ( $0.13$ ). The total effect of VPD on GEP ( $-0.51$ ) and NEE ( $-0.44$ ) under light saturated conditions is stronger than the other

**Table 2**

The annual mean and standard deviation of net ecosystem exchange (NEE), gross ecosystem productivity (GEP), and ecosystem respiration (RE) in units of  $\text{g C m}^{-2} \text{ y}^{-1}$  from tropical forest eddy covariance sites in the LaThuile and FLUXNET2015 eddy covariance databases. \* indicates that measurements of subcanopy  $\text{CO}_2$  storage were included in the NEE calculation in the LaThuile or FLUXNET2015 databases. Note that AU-Rob only includes one year of data and standard deviation could not be calculated. Values refer to measurement from the FLUXNET2015 when observations were available from both databases, i.e. we study the FLUXNET2015 values when data are available from both datasets because the time series are longer.

Sites	LaThuile			FLUXNET2015				
	NEE	Nighttime flux partitioning approaches		NEE	Nighttime flux partitioning approaches		Daytime flux partitioning approaches	
		GEP	RE		GEP	RE	GEP	RE
AU-Rob	–	–	–	–744	1994	1250	2112	1547
BR-Ban	$-1190 \pm 172$	$2623 \pm 202$	$1433 \pm 374$	–	–	–	–	–
BR-Cax	$-1002 \pm 88$	$2791 \pm 360$	$1788 \pm 419$	–	–	–	–	–
BR-Ji2	$-733 \pm 124$	$2990 \pm 154$	$2257 \pm 278$	–	–	–	–	–
BR-Ma2	$-953 \pm 151$	$2515 \pm 604$	$1578 \pm 487$	–	–	–	–	–
BR-Sa1*	–	–	–	$-57 \pm 197$	$3425 \pm 365$	$3391 \pm 227$	$3634 \pm 599$	$3953 \pm 649$
BR-Sa3*	–	–	–	$-171 \pm 328$	$3234 \pm 505$	$3033 \pm 745$	$3348 \pm 239$	$3483 \pm 504$
GF-Guy*	–	–	–	$-157 \pm 86$	$3720 \pm 223$	$3560 \pm 222$	$3637 \pm 222$	$3426 \pm 269$
GH-Ank*	–	–	–	$-768 \pm 223$	$2825 \pm 715$	$2009 \pm 508$	$2776 \pm 475$	$2250 \pm 286$
ID-Pag*	$375 \pm 179$	$3209 \pm 177$	$3584 \pm 2$	–	–	–	–	–
MY-PSO*	–	–	–	$-999 \pm 110$	$2495 \pm 120$	$1510 \pm 76$	$2608 \pm 169$	$1629 \pm 188$
PA-SPn*	–	–	–	$-600 \pm 248$	$2328 \pm 376$	$1679 \pm 128$	$2215 \pm 22$	$1667 \pm 39$
VU-Coc	$-367 \pm 264$	$3505 \pm 74$	$3138 \pm 338$	–	–	–	–	–

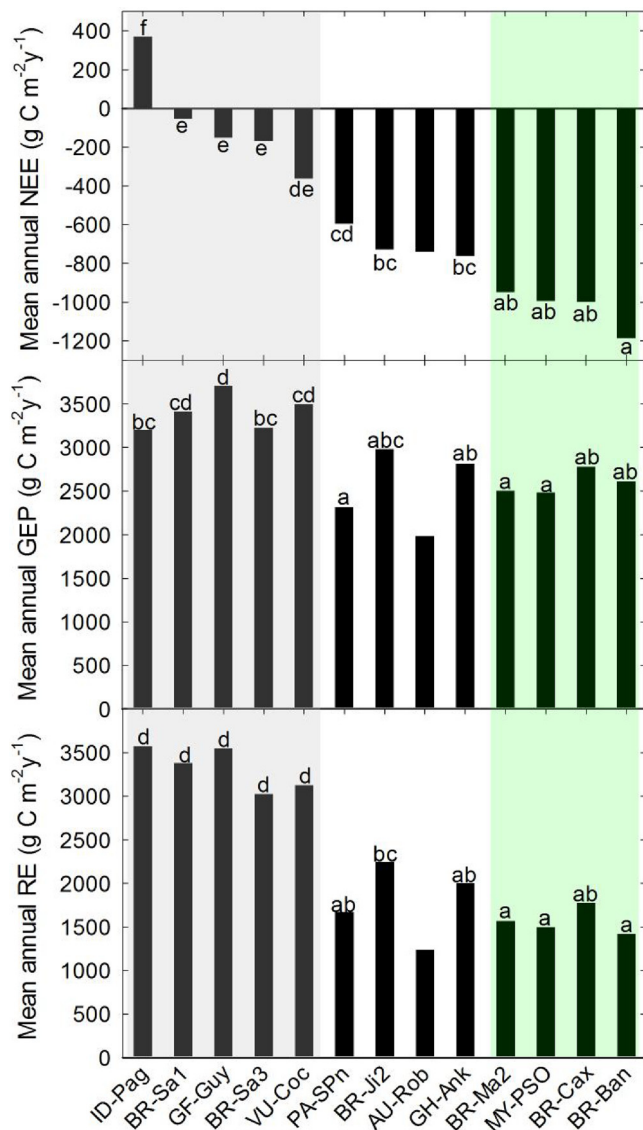


**Fig. 5.** Mean annual net ecosystem exchange (NEE), gross ecosystem productivity (GEP) and ecosystem respiration (RE) during the available observation period for the eddy covariance research sites described in Table 1 (see also Table 2). Gray shading represents the sites identified by the least-significant difference test ( $P < 0.05$ ) for multiple comparisons as having a net C sink of greater than  $-400 \text{ g C m}^{-2} \text{ y}^{-1}$ ; green shading represents sites with a NEE of less than  $-900 \text{ g C m}^{-2} \text{ y}^{-1}$ , while white represents sites with NEE between  $-400$  and  $-900 \text{ g C m}^{-2} \text{ y}^{-1}$ . The different lowercase letters indicate the significant difference ( $P < 0.05$ ) between carbon flux at different sites and are marked as a, b, c, d, e and f, successively. (For interpretation of the references to colour in this figure legend, the reader is referred to the web version of this article.)

indicators (Tables 3 & 4). The path analysis also indicates that  $T_a$  has a strong indirect effect on GEP ( $-0.36$ , Table 3) and NEE ( $-0.29$ , Table 4) due to its impact on VPD.

Path values from individual sites point to differences in the relationship between micrometeorological variables and carbon fluxes under light saturated conditions. AU-Rob, near the tropical/subtropical forest ecotone, has positive direct and total effects on GEP and NEE by SWC (0.31 and greater) that balances the negative effect of VPD ( $-0.37$  to  $-0.38$ ).  $T_a$  has no significant direct effect on GEP at 3 of the seven sites (4 sites for NEE) that measured both SWC and VPD, but  $T_a$  had a total effect on GEP that exceeded that of VPD at BR-Sa3 and ID-Pag (and a larger total effect on NEE at BR-Sa3). The strong relationships between  $T_a$  and VPD (0.83–0.87, Table A4) lead to large indirect effects on

GEP and NEE. SWC exerted a strong positive influence on GEP (0.71) and NEE (0.67) in the regrowing tropical forest PA-SPn.

### 3.5. Projected future climate conditions

Climate projections from 13 general circulation models (CMIP5) under RCP 8.5 suggest that many current tropical rainforest sites on the cooler end of the current temperature range are likely to reach a climate space similar to present-day warmer sites by the year 2050, and warmer sites will reach a climate space not currently experienced (Fig. 8).  $T_a$  and VPD have increased from the 1950s until the present at the study sites and are projected to increase further by the year 2050 (Fig. 8). The cooler AU-Rob ecosystem is projected to have a mean  $T_a$  on the order of  $24.5 \text{ }^\circ\text{C}$  by 2050, approaching the mean annual  $T_a$  of many study sites at the present (approximately  $25\text{--}26 \text{ }^\circ\text{C}$ , Fig. 4a). Many other ecosystems are projected to reach mean annual  $T_a$  values of  $30 \text{ }^\circ\text{C}$  or greater, which is not observed across any study sites at the present (Fig. 4a). Most sites are projected to have annual average VPD of  $> 10 \text{ hPa}$ , the point at which stomatal conductance often responds to VPD (Körner, 1995; Lasslop et al., 2010; Oren et al., 1999), noting that some of the drier ecosystems (e.g. BR-Ban on the tropical rainforest/cerrado ecotone) currently experience such conditions on an annual or monthly basis (Fig. 4d) and that GEP appears to respond to VPD at values below  $10 \text{ hPa}$  across the study ecosystems under light-saturated conditions (Figs. 6 and 7).

## 4. Discussion

### 4.1. Surface-atmosphere carbon dioxide flux in tropical rainforests

The broad definition of tropical rainforests applied in this study – including both managed and unmanaged ecosystems – leads to a large diversity of ecosystems with diverse ecosystem-atmosphere exchange of  $\text{CO}_2$ , but with largely consistent patterns with respect to micro-meteorological variability and measurement methodology. The five ecosystems that are estimated to have greater carbon uptake (with the magnitude of GEP greater than  $3000 \text{ g C m}^{-2} \text{ y}^{-1}$ ) sequester less carbon – or even lose it – on an annual basis because RE likewise tends to be large (Fig. 5). This apparent negative relationship between GEP and NEE should be critically examined against the observation that tower sites which were able to calculate NEE as the combination of subcanopy storage and eddy flux had higher magnitudes of GEP and RE and lower magnitudes of NEE (Table 1, Fig. 5). These findings may have implications for approaches that seek to upscale tower-based observations to larger regions given that the inclusion of subcanopy storage was related to a decrease in the magnitude of the measured C sink.

Carbon dioxide storage can dominate surface-atmosphere  $\text{CO}_2$  exchange over parts of the diurnal cycle (Malhi et al., 1998), particularly during the early morning, late evening and night (i.e. often during periods in which the NEE fluxes are used for gapfilling and partitioning algorithms). Given the importance of subcanopy  $\text{CO}_2$  storage measurements to net surface-atmosphere  $\text{CO}_2$  exchange in tropical rainforests (Araújo et al., 2002; Hayek et al., 2018; Hutrya et al., 2008), methodological differences among sites should be investigated to reduce uncertainties associated with NEE, GEP, and RE estimates. Additionally, careful consideration should be taken by users of tropical flux data to ensure robustness of results in the face of these uncertainties. Note that due to the small number of sites considered here (13 total), which limits statistical analysis and the diversity of ecosystems in question, we caution against making categorical statements about the cause of the finding that sites with high GEP have less net  $\text{CO}_2$  uptake. To illustrate this point, VU-Coc showed high GEP and RE, leading to a relatively weak net C sink, and was unable to provide subcanopy storage measurements. This can be attributed in part to the fact that seasonal cycles of net primary productivity of this coconut palm canopy are driven by fruit development; fruits accounted for 46%



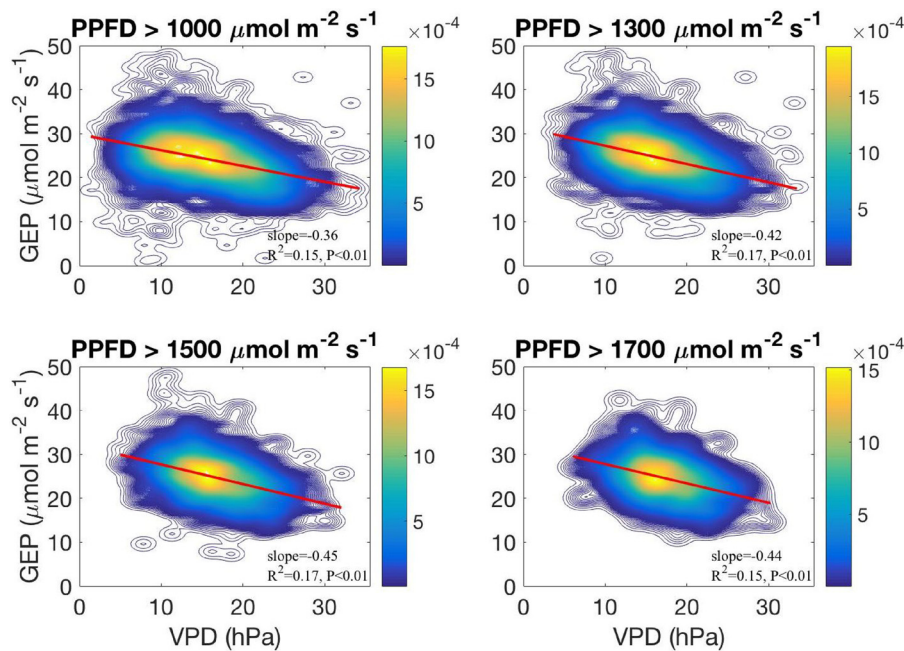


Fig. 6. The relationship between vapor pressure deficit (VPD) and gross ecosystem productivity (GEP) as represented by a two-dimensional kernel density estimate (“heat map”) for all half-hourly observations that passed FLUXNET quality control tests under different PPF thresholds for the Indonesia-Palangkaraya (ID-Pag) tropical peat forest ecosystem, taken as an example for all other sites. The color bar denotes the probability of finding a value within a given pixel and slopes are in units of  $\mu\text{mol CO}_2 \text{m}^{-2} \text{s}^{-1} \text{hPa}^{-1}$  from regression lines (red) calculated using ordinary least squares regression. (For interpretation of the references to colour in this figure legend, the reader is referred to the web version of this article.)

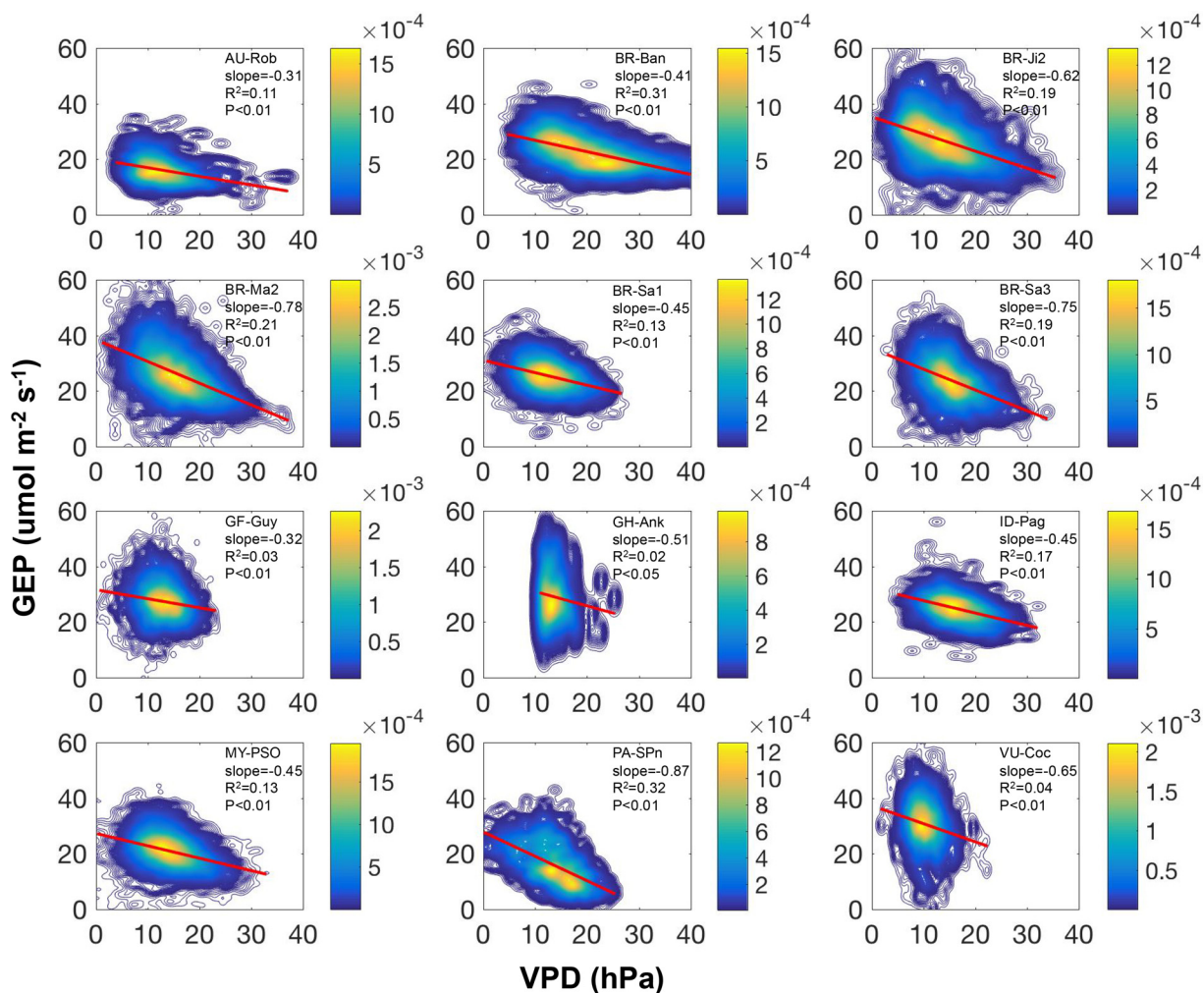


Fig. 7. The relationship between vapor pressure deficit (VPD) and gross ecosystem productivity (GEP) as represented by a two-dimensional kernel density estimate (“heat map”) for all half-hourly observations that passed FLUXNET quality control thresholds for different sites, choosing also values for which PPF  $> 1500 \mu\text{mol m}^{-2} \text{s}^{-1}$  following Wu et al., (2017) to include only periods with light-saturated conditions (Fig. 6). The color bar denotes the probability of finding a value within a given pixel and slopes are in units of  $\mu\text{mol CO}_2 \text{m}^{-2} \text{s}^{-1} \text{hPa}^{-1}$ .

**Table 3**

Standardized effect of air temperature ( $T_a$ ), vapor pressure deficit (VPD) and soil water content (SWC) on gross ecosystem productivity (GEP) from the path analysis (Fig. A1) for all half-hourly observations that passed FLUXNET quality control thresholds for different sites, choosing also values for which PPFD > 1500  $\mu\text{mol m}^{-2} \text{s}^{-1}$  to include only periods with light-saturated conditions. ns means insignificant paths ( $P > 0.05$ ).

Site	Direct effect on GEP			Indirect effect on GEP			Total effect on GEP		
	$T_a$	VPD	SWC	$T_a$	VPD	SWC	$T_a$	VPD	SWC
AU-Rob	0.28	-0.38	0.37	-0.36	-0.04	-0.08	-0.08	-0.42	0.41
BR-Sa3	-0.12	-0.35	ns	-0.29	ns	0.11	-0.41	-0.35	0.08
GF-Guy	ns	-0.22	0.06	-0.21	-0.01	0.02	-0.21	-0.22	0.08
ID-Pag	ns	-0.50	-0.31	-0.42	0.16	0.26	-0.42	-0.35	-0.05
MY-PSO	0.27	-0.57	0.09	-0.51	-0.02	0.09	-0.24	-0.59	0.25
PA-SPn	ns	-0.15	0.61	-0.03	-0.43	0.11	-0.03	-0.58	0.71
VU-Coc	0.14	-0.18	0.05	-0.02	-0.02	0.10	0.11	-0.20	0.12
All	0.28	-0.54	-0.31	-0.36	0.03	0.05	-0.08	-0.51	-0.25

**Table 4**

Standardized effect of air temperature ( $T_a$ ), vapor pressure deficit (VPD) and soil water content (SWC) on net ecosystem exchange (NEE) from the path analysis (Fig. A1) for all half-hourly observations that passed FLUXNET quality control thresholds for different sites, choosing also values for which PPFD > 1500  $\mu\text{mol m}^{-2} \text{s}^{-1}$  to include only periods with light-saturated conditions. ns means insignificant paths ( $P$ -value > 0.05).

Sites	Direct effect on -NEE			Indirect effect on -NEE			Total effect on -NEE		
	$T_a$	VPD	SWC	$T_a$	VPD	SWC	$T_a$	VPD	SWC
AU-Rob	ns	-0.37	0.31	-0.33	-0.04	0.04	-0.33	-0.40	0.35
BR-Sa3	-0.12	-0.27	ns	-0.23	ns	0.09	-0.34	-0.27	0.09
GF-Guy	-0.18	-0.15	-0.03	-0.11	ns	0.10	-0.29	-0.15	0.07
ID-Pag	ns	-0.58	-0.17	-0.49	0.09	0.30	-0.49	-0.49	0.12
MY-PSO	0.22	-0.56	ns	-0.48	ns	0.10	-0.27	-0.56	0.10
PA-SPn	ns	-0.25	0.49	-0.08	-0.35	0.18	-0.08	-0.60	0.67
VU-Coc	ns	-0.19	-0.08	-0.06	0.03	0.07	-0.06	-0.16	-0.01
All	0.13	-0.45	-0.08	-0.29	0.01	0.04	-0.16	-0.44	-0.04

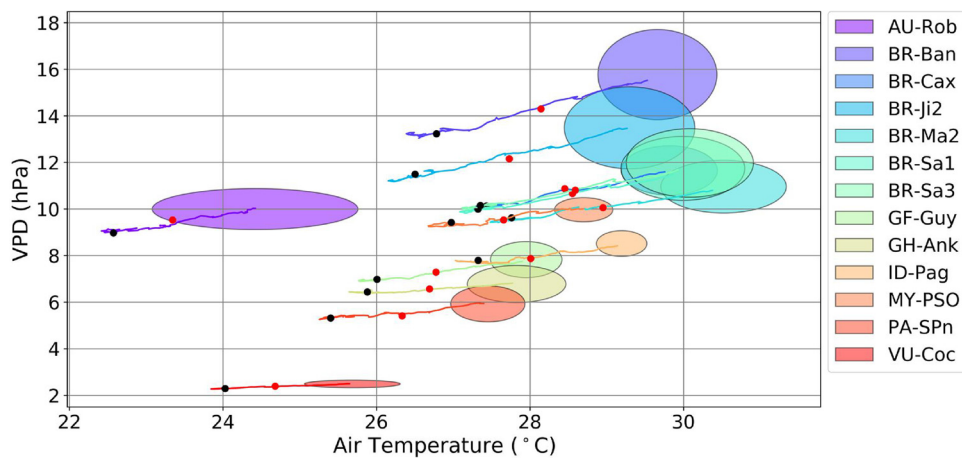


**Fig. 8.** Future climate projections from the ensemble mean of 13 CMIP5 models for vapor pressure deficit (VPD) and air temperature ( $T_a$ ) for the representative concentration pathway (RCP) 8.5. The black dots represent the 1950 average; the red dots represent the 2017 average while the lines represent the time series from 1950 to 2050, smoothed with a five-year moving average. As a consequence, dots that reflect individual years may not perfectly align with lines. The oval shadings indicate the standard deviation of the 2050 projected climate regime. (For interpretation of the references to colour in this figure legend, the reader is referred to the web version of this article.)

of tree net primary productivity at Vu-Coc (Navarro et al., 2008). Conversely, some non-agricultural sites that provided subcanopy C storage measurements (e.g. GH-Ank and PA-SPn) did not have high magnitudes of GEP and RE compared to other study ecosystems, leading to a relatively weak net C sink (Table 1, Fig. 5). In other words, methodological differences alone cannot fully explain the pattern of NEE across sites, highlighting the role of environmental and ecological controls on NEE. Other unmeasured state factors such as soil fertility, forest composition, topography and disturbance history, can also strongly influence tropical rainforest C cycling (e.g. Aiba and Kitayama,

(1999); Asner et al., (2015); Cleveland et al., (2011); Fuentes et al., (2016); Paoli et al., (2008); Raich et al., (1997)). Resolving other controls on rates of ecosystem C exchange will require more holistic biogeochemical research alongside field inventories of tropical rainforest C budgets for an improved understanding of the mechanisms that result in different surface-atmosphere C fluxes amongst tropical rainforests.

This study also found that RE at BR-Sa1 estimated from daytime partitioning approaches was larger than that of nighttime partitioning approaches by 560  $\text{g C m}^{-2} \text{y}^{-1}$  on average ( $P < 0.05$ ). Previous work

at this site demonstrated that the choice of  $u_*$  threshold can change inferred NEE from a C sink to a C source (Hayek et al., 2018; Miller et al., 2004; Saleska et al., 2003). Nighttime partitioning approaches use nighttime RE observations under conditions of sufficient  $u_*$  to model RE during daytime and thus estimate GEP by the difference between modeled RE and measured NEE while daytime flux partitioning approaches is based on daytime data, which are used to parameterize a model to estimate GEP and RE. If we assume RE based on daytime flux measurements represent an improvement (Lasslop et al., 2010), both RE and GEP estimated from nighttime partitioning approaches may be underestimated. Small changes in the approach used to derive component fluxes has a substantial impact on their estimates, especially in tropical rainforests where GEP and RE are characteristically of large magnitude.

#### 4.2. Responses of tropical rainforest carbon flux to environmental drivers

High rainfall and warm temperatures consistently enhance both aboveground net primary productivity and decomposition at tropical rainforest sites (Cusack et al., 2009; Salinas et al., 2011; Taylor et al., 2017) by maximizing decomposer activity and promoting physical leaching of forest floor material (Cleveland et al., 2010; Wieder et al., 2009). Further increases in  $T_a$  translate into an increase in VPD if atmospheric humidity remains constant, and VPD serves as a strong control over GEP (Kiew et al., 2018; Wu et al., 2017). As a consequence, the ability of tropical rainforest trees to acclimate to both  $T_a$  and VPD should be investigated to understand how they may (or may not) adapt to projected global changes over the coming decades. Recent studies have also emphasized the important role of canopy surface temperature in constraining GEP in tropical forests (Pau et al., 2018). Five of the study ecosystems provided outgoing longwave radiation flux observations by which radiometric surface temperature can be estimated using the Stefan-Boltzmann law, but it is difficult to distinguish canopy surface temperature from the temperature of other elements in the ecosystem that tend to be warmer than leaves during the day (like tree bark) or cooler like soil. Integrating phenological cameras that can observe the thermal (Pau et al., 2018), visible (Lopes et al., 2016; Richardson et al., 2009), and near infra-red bands (Richardson et al., 2009) with existing eddy covariance measurements is a logical way forward for understanding spatial and temporal processes that are important for flux dynamics.

To the extent that the response of GEP to VPD reflects canopy isohydricity through its relationship to leaf water potential (Martinez-Vilalta et al., 2014; Matheny et al., 2017), our results suggest that the trees at different sites may have varying degrees of isohydricity that may influence their response to predicted increases in VPD (Fig. 8). Isohydricity is strongly related to canopy height (Giardina et al., 2018; Konings and Gentine, 2016), as is reference canopy conductance (conductance when VPD = 10 hPa, Novick et al., (2009)). From the observations, it is unclear why the 13 different tropical rainforest canopies exhibited different responses of GEP to increases in VPD (Fig. 7) as the slope of the relationships were unrelated to other aspects of the soil-vegetation-atmosphere hydraulic transport system including rooting depth and SWC (data not shown). Path analysis indicated that VPD tended to have a stronger total (negative) effect on GEP and NEE under light-saturated conditions than did  $T_a$  or SWC across most study ecosystems (Tables 3 and 4), in agreement with the findings of Wu et al., (2017) and Kiew et al., (2018). The negative relationship between flux and  $T_a$  is mainly because  $T_a$  is closely related with VPD (Table A4), which led to large indirect (negative) effects on GEP or NEE. In other words, VPD is mainly responsible for the decline in light-

saturated GEP and NEE based on the path analysis, but this does not preclude the importance of  $T_a$  (especially via its relationship to VPD and surface temperature) and SWC on controlling carbon fluxes in tropical rainforest ecosystems, noting also that we were able to study the interplay between hydraulic variables and carbon fluxes at only seven of the thirteen study sites due to data availability constraints (Tables 3 and 4).

#### 4.3. Future directions

Future studies should continue research on tropical tree sensitivity to hydrologic stress both through decreases in SWC and increases VPD, and study whether and how tropical trees may acclimate to VPD as well as canopy surface temperature (Pau et al., 2018), which may limit responses to future climate increases (Kutsch et al., 2001; Marchin et al., 2016). Models consistently estimate future increases in  $T_a$  and VPD at the study sites (Fig. 8), albeit with a considerable uncertainty range across the CMIP5 models. Ecosystems with already higher VPD are expected to experience the strongest VPD increase. No such agreement is found for SWC given the challenges of estimating future precipitation (Novick et al., 2016), highlighting the importance to measure and study both VPD and soil moisture trends in concert to understand how tree physiology is impacted by water supply (via SWC) and demand (via VPD). Moreover, increasing  $CO_2$  levels will also impact stomatal aperture and thus GEP (Swann et al., 2016), highlighting the need to study all climate change effects on GEP in concert.

Results also demonstrate that flux measurement methodology in tropical rainforest ecosystems is an important avenue of future research (Hayek et al., 2018). The impact of nighttime gapfilling on carbon fluxes partitioning (as discussed in Section 4.1) is further exacerbated by tropical rainforests' characteristically large plant area indices and the presence of large within-canopy air spaces that result in decoupling between above and below-canopy flows. Recent studies have demonstrated the utility of using the variance of vertical wind velocity ( $\sigma_w$ ) rather than  $u_*$  as an improved criterion for approximating the coupling between the within and above-canopy air space in forested canopies for determining the quality of flux measurements (Santana et al., 2018), especially at night (Acevedo et al., 2009; Jocher et al., 2017; Thomas et al., 2013). Hayek et al., (2018) reiterated the importance of sub-canopy drainage and introduced approaches to account for potential "missing"  $CO_2$  storage. Results in the present manuscript agree with the argument that alternative flux partitioning and eddy covariance processing techniques should be explored across different tropical forests to better-constrain their role in the regional and global C cycle.

## 5. Conclusions

Eddy covariance measurements suggest that tropical rainforest canopies exhibit a wide range of NEE values that range from carbon source to sink, but these estimates are sensitive to flux measurement methodology. Sites that included subcanopy  $CO_2$  storage values reported characteristically higher magnitudes of GEP (greater than  $3000 \text{ g C m}^{-2} \text{ y}^{-1}$ ) and RE, and consequently lower NEE, characteristically between approximately  $400 \text{ g C m}^{-2} \text{ y}^{-1}$  (i.e. a  $CO_2$  source to the atmosphere) and about  $-400 \text{ g C m}^{-2} \text{ y}^{-1}$ . This highlights the importance of standardized processing of biosphere-atmosphere flux measurements, which is particularly challenging in tropical forests given logistical considerations. Such estimates will serve to increase the confidence in studies that assess ecosystem and environmental variability as drivers for variations in NEE, GEP, and RE. That being said,  $CO_2$  storage measurements alone cannot fully explain the differences in NEE, GEP,

and RE amongst sites, demonstrating the importance of ecological differences amongst tropical forest ecosystems. Our results emphasize the importance and diversity of tropical rainforest carbon flux responses to atmospheric water deficit, and future studies should investigate the acclimation of mature tropical trees to increases in VPD in addition to  $T_a$ . Combined, our results highlight the importance of continued research into the biosphere-atmosphere exchange of  $CO_2$  in tropical forests, especially as fewer observations are available in more recent years than in the past.

Logistical challenges of making ecosystem-scale measurements on a quasi-continuous basis at remote research sites with tall canopies that require considerable infrastructure and reliable power systems persist. Recent and forthcoming research initiatives including the Amazon Tall Tower Observatory (ATTO, see [Andreae et al., \(2015\)](#)), Next Generation Ecosystem Experiments—Tropics (NGEE-Tropics, [Chambers et al., \(2014\)](#)) and associated Amazon Free Atmosphere Carbon Enrichment facility (AmazonFACE, [Norby et al. \(2015\)](#)) suggest that more eddy covariance and model estimates of tropical rainforest GEP and RE will be available in the future if funding is sustained. Such investments will help stem the decline in tropical rainforest flux data availability ([Fig. 3](#)), but global initiatives must be undertaken to improve our ability to observe the carbon dynamics of tropical ecosystems across different regions.

### Acknowledgements

PCS and JDF acknowledges funding support from the U.S. Department of Energy as part of the GoAmazon project (Grant

SC0011097). PCS additionally acknowledges the U.S. National Science Foundation grants 1552976 and 1702029, and The Graduate School at Montana State University. ZF is supported by the China Scholarship Council and National Natural Science Foundation of China (31625006). This work used eddy covariance data acquired and shared by the FLUXNET community, including the AmeriFlux, AfriFlux, AsiaFlux, CarboAfrica, LBA, and TERN- OzFlux networks. The FLUXNET eddy covariance data processing and harmonization was carried out by the ICOS Ecosystem Thematic Center, AmeriFlux Management Project and Fluxdata project of FLUXNET, with the support of CDIAC, and the OzFlux, ChinaFlux and AsiaFlux offices. The Guyaflux program belongs to the SOERE F-ORE-T which is supported annually by Ecofor, Allenvi and the French national research infrastructure ANAEE-F. The Guyaflux program also received support from the "Observatoire du Carbone en Guyane" and an "investissement d'avenir" grant from the Agence Nationale de la Recherche (CEBA, ref ANR-10-LABX-25-01). Funding for the site PA-SPn was provided by the North-South Centre of ETH Zurich. We acknowledge the World Climate Research Programme's Working Group on Coupled Modeling for the CMIP and thank the climate modeling groups for producing and making available their model output. For CMIP, the U.S. Department of Energy's Program for Climate Model Diagnosis and Intercomparison provides coordinating support and led development of software infrastructure in partnership with the Global Organization for Earth System Science Portals. Angela Tang and Taylor Rodenburg provided valuable comments to earlier drafts of this manuscript. We thank Dr. Tim Hill and two anonymous reviewers for their constructive comments on the manuscript.

### Appendix A

#### A1 Notes on the FLUXNET2015 C flux calculation

It is noteworthy that NEE is only approximately equal to RE minus GEP for daily data although NEE is equal to RE minus GEP for half-hourly data in FLUXNET 2015. In FLUXNET 2015, a reference NEE was selected on the basis of the Model Efficiency (identified with “\_REF” in the variable name). The extraction of NEE\_REF is done separately for each time aggregation and for this reason the  $u^*$  threshold associated to the NEE\_REF can change across time. The Model Efficiency calculation (which determines \_REF variables) is performed independently using variable  $u^*$  thresholds (NEE\_VUT\_REF, [Table A1](#)) and for each temporal aggregation. Therefore, percentile variables are re-ranked at each temporal aggregation, and reference values (\_REF) are recomputed, and should not be considered the same variable. For instance, NEE\_VUT\_REF at half-hourly resolution might have been generated using a different  $u^*$  threshold than NEE\_VUT\_REF at daily resolution. In this way, NEE is approximately but not exactly equal to RE minus GEP for yearly data in [Table 3](#) because annual NEE, RE and GEP were taken from the sum from daily data.

**Table A1**

A list of variables and their description and units, including the name of each variable in the LaThuile and FLUXNET2015 databases.

Variable	LaThuile	FLUXNET2015	Units	Description
NEE	NEE_f	NEE_VUT_REF	$\mu\text{mol CO}_2 \text{ m}^{-2} \text{ s}^{-1}$ or $\text{g C m}^{-2} \text{ y}^{-1}$	Net ecosystem exchange
GEP	GEP_f	GEP_NT_VUT_REF	$\mu\text{mol CO}_2 \text{ m}^{-2} \text{ s}^{-1}$ or $\text{g C m}^{-2} \text{ y}^{-1}$	Gross ecosystem productivity
RE	Reco	RECO_NT_VUT_REF	$\mu\text{mol CO}_2 \text{ m}^{-2} \text{ s}^{-1}$ or $\text{g C m}^{-2} \text{ y}^{-1}$	Ecosystem respiration
$T_a$	Ta_f	TA_F	$^{\circ}\text{C}$	Air temperature
VPD	VPD_f	VPD_F	hPa	Vapor pressure deficit
Precipitation	Precip_f	P_F	mm	Precipitation
$T_s$	Ts1_f	TS_F_MDS_1	$^{\circ}\text{C}$	Soil temperature (upper layer) *
SWC	SWC1_f	SWC_F_MDS_1	%	Soil water content (upper layer) †
PPFD	PPFD_f	PPFD_IN	$\mu\text{mol m}^{-2} \text{ s}^{-1}$	Photosynthetic photon flux density

\* Soil measurement depths vary.

**Table A2**

The 13 General Circulation Models (GCMs) from the Coupled Model Intercomparison Project - Phase 5 archive (CMIP5) used in the present analysis.

Model Name	Model Country	Developed by
<a href="#">ACCESS1_0</a>	Australia	Commonwealth Scientific and Industrial Research Organisation, Australia (CSIRO), and Bureau of Meteorology, Australia (BOM)
<a href="#">BNU-ESM</a>	China	College of Global Change and Earth System Science, Beijing Normal University, China
<a href="#">CNRM-CM5</a>	France	National Centre of Meteorological Research, France
<a href="#">CSIRO-Mk3-6-0</a>	Australia	Commonwealth Scientific and Industrial Research Organization/Queensland Climate Change Centre of Excellence, Australia
<a href="#">CanESM2</a>	Canada	Canadian Centre for Climate Modeling and Analysis
<a href="#">GFDL-CM3</a>	United States	National Oceanic and Atmospheric Administration Geophysical Fluid Dynamics Laboratory
<a href="#">GISS-E2-R</a>	United States	NASA Goddard Institute for Space Studies
<a href="#">IPSL-CM5A-LR</a>	France	Institut Pierre Simon Laplace, France
<a href="#">MIROC-ESM</a>	Japan	Japan Agency for Marine-Earth Science and Technology, Atmosphere and Ocean Research Institute (The University of Tokyo), and National Institute for Environmental Studies
<a href="#">MIROC5</a>	Japan	Atmosphere and Ocean Research Institute (The University of Tokyo), National Institute for Environmental Studies and Japan Agency for Marine-Earth Science and Technology
<a href="#">MPI-ESM-LR</a>	Germany	Max Planck Institute for Meteorology (MPI-M)
<a href="#">MRI-CGCM3</a>	Japan	Meteorological Research Institute, Japan
<a href="#">inmcm4</a>	Russia	Institute for Numerical Mathematics, Russia

**Table A3**

Results of a one-way analysis of variance (ANOVA) for mean comparisons of annual RE and GEP at BR-Sa1 using nighttime and daytime partitioning approaches. NT\_DT means nighttime partitioning approaches versus daytime partitioning approaches. Please see [Table A1](#) for abbreviations.

		Sum of Squares	df	Mean Square	F	Sig.
RE × NT_DT	Between Groups	1,423,608.758	1	1,423,608.758	6.026	0.026
	Within Groups	3780046.637	16	236252.915		
	Total	5203655.395	17			
GEP × NT_DT	Between Groups	196,991.091	1	196,991.091	0.801	0.384
	Within Groups	3932744.559	16	245796.535		
	Total	4129735.650	17			

**Table A4**

The covariance between air temperature ( $T_a$ ), vapor pressure deficit (VPD), and soil water content (SWC) at the study ecosystems during the measurement period as determined by path analysis ([Fig. A1](#)).

Site	Covariance		
	Ta-SWC	Ta-VPD	VPD-SWC
AU-Rob	-0.43	0.53	-0.11
BR-Sa3	-0.27	0.84	-0.23
GF-Guy	-0.49	0.83	-0.09
ID-Pag	-0.06	0.87	-0.51
MY-PSO	-0.24	0.86	-0.27
PA-SPn	0.04	0.33	-0.72
VU-Coc	0.24	0.2	-0.37
All	ns	0.66	-0.1

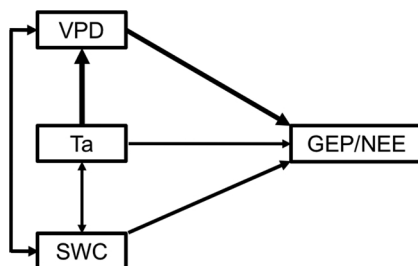


**Fig. A1.** A path diagram illustrating interactions between the micrometeorological variables  $T_a$ , VPD and SWC and their controls on GEP and NEE. We use half-hourly observations that passed FLUXNET quality control thresholds for different sites, choosing also values for which PFD > 1500  $\mu\text{mol m}^{-2} \text{s}^{-1}$  to include only periods with light-saturated conditions for the analysis. The thickness of each arrow indicates standardized correlation coefficients (path value) described in [Tables 3 and 4](#).

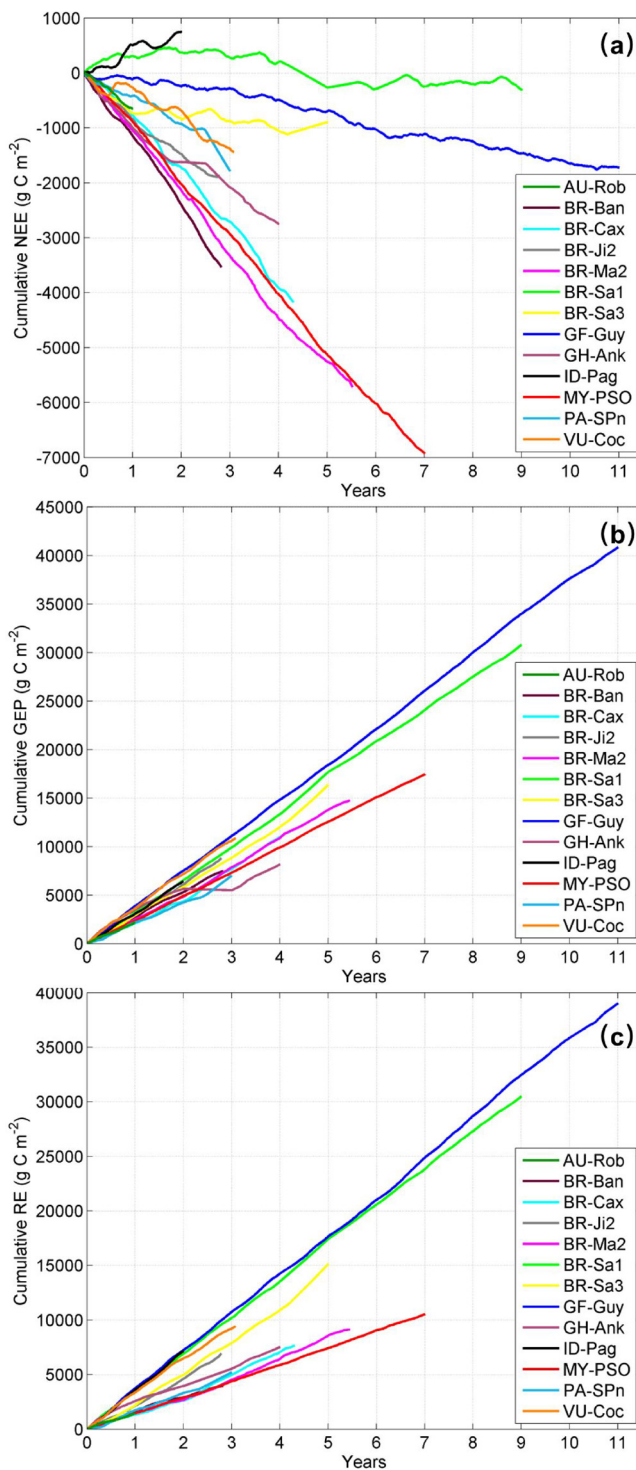


**Fig. A2.** The cumulative sum of net ecosystem exchange (NEE, a), gross ecosystem productivity (GEP, b) and ecosystem respiration (RE, c) using nighttime partitioning methods since the beginning of the measurements at the tropical forest eddy covariance research sites (see Table 1) using observations from the FLUXNET2015 database when possible and the LaThuile database when data were not available in FLUXNET2015 (Table 2).

**References**

Acevedo, O.C., Moraes, O.L.L., Degrazia, G.A., Fitzjarrald, D.R., Manzi, A.O., Campos, J.G., 2009. Is friction velocity the most appropriate scale for correcting nocturnal carbon dioxide fluxes? *Agric. For. Meteorol.* 149, 1–10. <https://doi.org/10.1016/j.agrformet.2008.06.014>.

Aguilos, M., Hérault, B., Burban, B., Wagner, F., Bonal, D., 2018. What drives long-term variations in carbon flux and balance in a tropical rainforest in French Guiana? *Agric. For. Meteorol.* 253–254, 114–123. <https://doi.org/10.1016/J.AGRFORMET.2018.02.009>.

Ahlström, A., Raupach, M.R., Schurgers, G., Smith, B., Armeth, A., Jung, M., Reichstein, M., Canadell, J.G., Friedlingstein, P., Jain, A.K., 2015. The dominant role of semi-arid ecosystems in the trend and variability of the land CO<sub>2</sub> sink. *Science* 348 (80), 895–899.

Aiba, S.I., Kitayama, K., 1999. Structure, composition and species diversity in an altitude-substrate matrix of rain forest tree communities on Mount Kinabalu. *Borneo. Plant Ecol.* 140, 139–157. <https://doi.org/10.1023/A:1009710618040>.

Andreae, M.O., Artaxo, P., Brandão, C., Carswell, F.E., Ciccioli, P., da Costa, A.L., Culf, A.D., Esteves, J.L., Gash, J.H.C., Grace, J., Kabat, P., Lelieveld, J., Malhi, Y., Manzi,

- A.O., Meixner, F.X., Nobre, A.D., Nobre, C., Ruivo, M.D.L.P., Silva-Dias, M.A., Stefani, P., Valentini, R., von Jönnemann, J., Waterloo, M.J., 2002. Biogeochemical cycling of carbon, water, energy, trace gases, and aerosols in Amazonia: the LBA-EUSTACH experiments. *J. Geophys. Res.* 107, 8066. <https://doi.org/10.1029/2001JD000524>.
- Andreea, M.O., Acevedo, O.C., Araújo, A., Artaxo, P., Barbosa, C.G.G., Barbosa, H.M.J., Brito, J., Carbone, S., Chi, X., Cintra, B.B.L., Da Silva, N.F., Dias, N.L., Dias-Júnior, C.Q., Ditas, F., Ditz, R., Godoi, A.F.L., Godoi, R.H.M., Heimann, M., Hoffmann, T., Kesselmeier, J., Könemann, T., Krüger, M.L., Lavric, J.V., Manzi, A.O., Lopes, A.P., Martins, D.L., Mikhailov, E.F., Moran-Zuloaga, D., Nelson, B.W., Nölscher, A.C., Santos Nogueira, D., Piedade, M.T.F., Pöhlker, C., Pöschl, U., Quesada, C.A., Rizzo, L.V., Ro, C.U., Ruckteschler, N., Sá, L.D.A., De Oliveira Sá, M., Sales, C.B., Dos Santos, R.M.N., Saturno, J., Schöngart, J., Sörgel, M., De Souza, C.M., De Souza, R.A.F., Su, H., Targhetta, N., Tóta, J., Trebs, I., Trumbore, S., Van Eijck, A., Walter, D., Wang, Z., Weber, B., Williams, J., Winderlich, J., Wittmann, F., Wolff, S., Yáñez-Serrano, A.M., 2015. The Amazon Tall Tower Observatory (ATTO): overview of pilot measurements on ecosystem ecology, meteorology, trace gases, and aerosols. *Atmos. Chem. Phys.* 15, 10723–10776. <https://doi.org/10.5194/acp-15-10723-2015>.
- Araújo, A.C., Nobre, A.D., Kruijt, B., Elbers, J.A., Dallara, R., Stefani, P., Von Randow, C., Manzi, A.O., Culf, A.D., Gash, J.H.C., Valentini, R., Kabat, P., 2002. Comparative measurements of carbon dioxide fluxes from two nearby towers in a central Amazonian rainforest: The Manaus LBA site. *J. Geophys. Res.* 107, 8090. <https://doi.org/10.1029/2001JD000676>.
- Asner, G.P., Anderson, C.B., Martin, R.E., Tupayachi, R., Knapp, D.E., Sinca, F., 2015. Landscape biogeochemistry reflected in shifting distributions of chemical traits in the Amazon forest canopy. *Nat. Geosci.* 8, 567–573.
- Asner, G.P., Martin, R.E., Knapp, D.E., Tupayachi, R., Anderson, C.B., Sinca, F., Vaughn, N.R., Llactayo, W., 2017. Airborne laser-guided imaging spectroscopy to map forest trait diversity and guide conservation. *Science* 355 (80), 385–389.
- Avissar, R., Werth, D., 2005. Global hydroclimatology teleconnections resulting from tropical deforestation. *J. Hydrometeorol.* 6, 134–145.
- Baccini, A., Walker, W., Carvalho, L., Farina, M., Sulla-Menashe, D., Houghton, R.A., 2017. Tropical forests are a net carbon source based on aboveground measurements of gain and loss. *Science* 358 (80), 230–234.
- Belelli Marchesini, L., Bombelli, A., Chiti, T., Consalvo, C., Forgiione, A., Grieco, E., Mazzenga, F., Papale, D., Stefani, P., Vittorini, E., Zompanti, R., Valentini, R., 2008. Ankasa flux tower: a new research facility for the study of the carbon cycle in a primary tropical forest in Africa. *Proceedings of the Open Science Conference on Africa and Carbon Cycle: The CarboAfrica Project*.
- Beringer, J., Hutley, L.B., McHugh, I., Arndt, S.K., Campbell, D., Cleugh, H.A., Cleverly, J., Resco de Dios, V., Eamus, D., Evans, B., Ewenz, C., Grace, P., Griebel, A., Haverd, V., Hinko-Najera, N., Huete, A., Isaac, P., Kanniah, K., Leuning, R., Liddell, M.J., Macfarlane, C., Meyer, W., Moore, C., Pendall, E., Phillips, A., Phillips, R.L., Prober, S.M., Restrepo-Coupe, N., Rutledge, S., Schroder, I., Silberstein, R., Southall, P., Yee, M.S., Tapper, N.J., van Gorsel, E., Vote, C., Walker, J., Wardlaw, T., 2016. An introduction to the Australian and New Zealand flux tower network – OzFlux. *Biogeosciences* 13, 5895–5916. <https://doi.org/10.5194/bg-13-5895-2016>.
- Bonal, D., Bosc, A., Ponton, S., Goret, J.-Y., Burban, B.T., Gross, P., Bonnefond, J.M.J.-M., Elbers, J., Longdoz, B., Epron, D., Guehl, J.M.J.-M., Granier, A., 2008. Impact of severe dry season on net ecosystem exchange in the Neotropical rainforest of French Guiana. *Glob. Chang. Biol.* 14, 1917–1933. <https://doi.org/10.1111/j.1365-2486.2008.01610.x>.
- Borma, L.S., da Rocha, H.R., Cabral, O.M., von Randow, C., Collicchio, E., Kurzatkowski, D., Brügger, P.J., Freitas, H., Tannus, R., Oliveira, L., Rennó, C.D., Artaxo, P., 2009. Atmosphere and hydrological controls of the evapotranspiration over a floodplain forest in the Bananal Island region, Amazonia. *J. Geophys. Res. Biogeosci.* 114. <https://doi.org/10.1029/2007JG000641>.
- Bradford, M.G., Metcalfe, D.J., Ford, A., Liddell, M.J., McKeown, A., 2014. Floristics, stand structure and aboveground biomass of a 25-ha rainforest plot in the Wet Tropics of Australia. *J. Trop. For. Sci.* 543–553.
- Braga, N., da, S., Vitória, A.P., Souza, G.M., Barros, C.F., Freitas, L., 2016. Weak relationships between leaf phenology and isohyric and anisohyric behavior in lowland wet tropical forest trees. *Biotropica* 48, 453–464. <https://doi.org/10.1111/btp.12324>.
- Carswell, F.E., Costa, A.L., Palheta, M., Malhi, Y., Meir, P., Costa, J.D.P.R., Ruivo, M.D.L., Leal, L.D.S.M., Costa, J.M.N., Clement, R.J., Grace, J., 2002. Seasonality in CO<sub>2</sub> and H<sub>2</sub>O flux at an eastern Amazonian rain forest. *J. Geophys. Res. D Atmos.* 107. <https://doi.org/10.1029/2000JD000284>.
- Chambers, J.Q., Tribuzy, E.S., Toledo, L.C., Crispim, B.F., Higuchi, N., dos Santos, J., Araújo, A.C., Kruijt, B., Nobre, A.D., Trumbore, S.E., 2004. Respiration from a tropical forest ecosystem: partitioning of sources and low carbon use efficiency. *Ecol. Appl.* 14, 72–88.
- Chambers, J., Davies, S., Koven, C., Kueppers, L., Leung, R., McDowell, N., Norby, R., Rogers, A., 2014. Next Generation Ecosystem Experiment (NGEE) Tropics. US DOE NGEETrop. white paper. Next Generation Ecosystem Experiment (NGEE) Tropics. US DOE NGEETrop. white paper.
- Chiti, T., Certini, G., Grieco, E., Valentini, R., 2010. The role of soil in storing carbon in tropical rainforests: the case of Ankasa Park, Ghana. *Plant Soil* 331, 453–461. <https://doi.org/10.1007/s11104-009-0265-x>.
- Cleveland, C.C., Wieder, W.R., Reed, S.C., Townsend, A.R., 2010. Experimental drought in a tropical rain forest increases soil carbon dioxide losses to the atmosphere. *Ecology* 91, 2313–2323. <https://doi.org/10.1890/09-1582.1>.
- Cleveland, C.C., Townsend, A.R., Taylor, P., Alvarez-Clare, S., Bustamante, M.M.C., Chuyong, G., Dobrowski, S.Z., Grierson, P., Harms, K.E., Houlton, B.Z., Marklein, A., Parton, W., Porder, S., Reed, S.C., Sierra, C.A., Silver, W.L., Tanner, E.V.J., Wieder, W.R., 2011. Relationships among net primary productivity, nutrients and climate in tropical rain forest: a pan-tropical analysis. *Ecol. Lett.* <https://doi.org/10.1111/j.1461-0248.2011.01658.x>.
- Cusack, D.F., Chou, W.W., Yang, W.H., Harmon, M.E., Silver, W.L., 2009. Controls on long-term root and leaf litter decomposition in neotropical forests. *Glob. Chang. Biol.* 15, 1339–1355. <https://doi.org/10.1111/j.1365-2486.2008.01781.x>.
- da Rocha, H.R., Manzi, A.O., Cabral, O.M., Miller, L.G., Goulden, M.L., Saleska, S.R., Coupe, N.R., Wofsy, S.C., Borma, L.S., Artaxo, R., Vourlitis, G., Nogueira, J.S., Cardoso, F.L., Nobre, A.D., Kruijt, B., Freitas, H.C., Von Randow, C., Aguiar, R.G., Maia, J.F., 2009. Patterns of water and heat flux across a biome gradient from tropical forest to savanna in Brazil. *J. Geophys. Res. Biogeosci.* 114. <https://doi.org/10.1029/2007JG000640>. G00B12.
- Dargie, G.C., Lewis, S.L., Lawson, I.T., Mitchard, E.T.A., Page, S.E., Bocko, Y.E., Ifo, S.A., 2017. Age, extent and carbon storage of the central Congo Basin peatland complex. *Nature* 542, 86–89.
- de Araújo, A.C., Dolman, A.J., Waterloo, M.J., Gash, J.H.C., Kruijt, B., Zanchi, F.B., de Lange, J.M.E., Stoevelaar, R., Manzi, A.O., Nobre, A.D., Looijens, R.N., Backer, J., 2010. The spatial variability of CO<sub>2</sub> storage and the interpretation of eddy covariance fluxes in central Amazonia. *Agric. For. Meteorol.* 150, 226–237. <https://doi.org/10.1016/j.agrformet.2009.11.005>.
- Dixon, R.K., Solomon, A.M., Brown, S., Houghton, R.A., Trexler, M.C., Wisniewski, J., 1994. Carbon pools and flux of global forest ecosystems. *Science* 263 (80), 185–190.
- Fisher, R.A., Williams, M., Do Vale, R.L., Da Costa, A.L., Meir, P., 2006. Evidence from Amazonian forests is consistent with isohyric control of leaf water potential. *Plant Cell Environ.* 29, 151–165. <https://doi.org/10.1111/j.1365-3040.2005.01407.x>.
- Foley, J.A., DeFries, R., Asner, G.P., Barford, C., Bonan, G., Carpenter, S.R., Chapin, F.S., Coe, M.T., Daily, G.C., Gibbs, H.K., Helkowski, J.H., Holloway, T., Howard, E.A., Kucharik, C.J., Monfreda, C., Patz, J.A., Prentice, I.C., Ramankutty, N., Snyder, P.K., 2005. Global consequences of land use. *Science* 309, 570–574.
- Fu, Z., Dong, J., Zhou, Y., Stoy, P.C., Niu, S., 2017. Long term trend and interannual variability of land carbon uptake—the attribution and processes. *Environ. Res. Lett.* 12, 14018.
- Fuentes, J.D., Chamecki, M., dos Santos, R.M.N., Von Randow, C., Stoy, P.C., Katul, G., Fitzjarrald, D., Manzi, A., Gerken, T., Trowbridge, A., Freire, L.S., Ruiz-Plancarte, J., Maia, J.M.F., Tóta, J., Dias, N., Fisch, G., Schumacher, C., Acevedo, O., Mercer, J.R., Yáñez-Serrano, A.M., 2016. Linking meteorology, turbulence, and air chemistry in the Amazon rain forest. *Bull. Am. Meteorol. Soc.* 97, 2329–2342. <https://doi.org/10.1175/BAMS-D-15-00152.1>.
- Gerken, T., Chamecki, M., Fuentes, J.D., 2017. Air-parcel residence times within forest canopies. *Boundary-Layer Meteorol.* 165, 29–54. <https://doi.org/10.1007/s10546-017-0269-7>.
- Giardina, F., Konings, A.G., Kennedy, D., Alemohammad, S.H., Oliveira, R.S., Uriarte, M., Gentine, P., 2018. Tall Amazonian forests are less sensitive to precipitation variability. *Nat. Geosci.* 11, 405–409. <https://doi.org/10.1038/s41561-018-0133-5>.
- Gibson, L., Lee, T.M., Koh, L.P., Brook, B.W., Gardner, T.A., Barlow, J., Peres, C.A., Bradshaw, C.J.A., Laurance, W.F., Lovejoy, T.E., Sodhi, N.S., 2011. Primary forests are irreplaceable for sustaining tropical biodiversity. *Nature* 478, 378–381. <https://doi.org/10.1038/nature10425>.
- Goulden, M.L., Miller, S.D., Da Rocha, H.R., 2006. Nocturnal cold air drainage and pooling in a tropical forest. *J. Geophys. Res. Atmos.* 111.
- Grace, J., Lloyd, J., McIntyre, J., Miranda, A., Meir, P., Miranda, H., Moncrieff, J., Massheder, J., Wright, I., Gash, J., 1995. Fluxes of carbon dioxide and water vapour over an undisturbed tropical forest in south-west Amazonia. *Glob. Chang. Biol.* 1, 1–12. <https://doi.org/10.1111/j.1365-2486.1995.tb00001.x>.
- Grace, J., Malhi, Y., Lloyd, J., McIntyre, J., Miranda, A.C., Meir, P., Miranda, H.S., 1996. The use of eddy covariance to infer the net carbon dioxide uptake of Brazilian rain forest. *Glob. Chang. Biol.* 2, 209–217.
- Grace, J., Nagy, L., Forsberg, B.R., Artaxo, P., 2016. The Amazon carbon balance: an evaluation of methods and results. *Interactions Between Biosphere, Atmosphere and Human Land Use in the Amazon Basin*. Springer, Berlin Heidelberg, pp. 79–100. [https://doi.org/10.1007/978-3-662-49902-3\\_5](https://doi.org/10.1007/978-3-662-49902-3_5).
- Hall, C.A.S., Tian, H., Qi, Y., Pontius, G., Cornell, J., 1995. Modelling spatial and temporal patterns of tropical land use change. *J. Biogeogr.* 22, 753–757. <https://doi.org/10.2307/2845977>.
- Hayek, M.N., Wehr, R., Longo, M., Hutryra, L.R., Wiedemann, K., Munger, J.W., Bonal, D., Saleska, S.R., Fitzjarrald, D.R., Wofsy, S.C., 2018. A novel correction for biases in forest eddy covariance carbon balance. *Agric. For. Meteorol.* 250–251, 90–101. <https://doi.org/10.1016/J.AGRFORMET.2017.12.186>.
- Hirano, T., Segah, H., Harada, T., Limin, S., June, T., Hirata, R., Osaki, M., 2007. Carbon dioxide balance of a tropical peat swamp forest in Kalimantan, Indonesia. *Glob. Chang. Biol.* 13, 412–425. <https://doi.org/10.1111/j.1365-2486.2006.01301.x>.
- Hirano, T., Jauhainen, J., Inoue, T., Takahashi, H., 2008. Controls on the carbon balance of tropical peatlands. *Ecosystems* 12, 873–887. <https://doi.org/10.1007/s10021-008-9209-1>.
- Hirano, T., Segah, H., Kusin, K., Limin, S., Takahashi, H., Osaki, M., 2012. Effects of disturbances on the carbon balance of tropical peat swamp forests. *Glob. Change Biol.* 18, 3410–3422.
- Huete, A.R., Didan, K., Shimabukuro, Y.E., Ratana, P., Saleska, S.R., Hutryra, L.R., Yang, W., Nemani, R.R., Myneni, R., 2006. Amazon rainforests green-up with sunlight in dry season. *Geophys. Res. Lett.* 33. <https://doi.org/10.1029/2005GL025583>. L06405.
- Huete, A.R., Restrepo-Coupe, N., Ratana, P., Didan, K., Saleska, S.R., Ichii, K., Panuthai, S., Gamo, M., 2008. Multiple site tower flux and remote sensing comparisons of tropical forest dynamics in Monsoon Asia. *Agric. For. Meteorol.* 148, 748–760. <https://doi.org/10.1016/j.agrformet.2008.01.012>.
- Hutryra, L.R., Munger, J.W., Saleska, S.R., Gottlieb, E., Daube, B.C., Dunn, A.L., Amaral, D.F., de Camargo, P.B., Wofsy, S.C., 2007. Seasonal controls on the exchange of carbon and water in an Amazonian rain forest. *J. Geophys. Res. Biogeosci.* 112. <https://doi.org/10.1029/2006JG000365>.





- Fitzjarrald, D.R., Goulden, M.L., Kruijt, B., Maia, J.M.F., Malhi, Y.S., Manzi, A.O., Miller, S.D., Nobre, A.D., von Randow, C., Sá, L.D.A., Sakai, R.K., Tota, J., Wofsy, S.C., Zanchi, F.B., Saleska, S.R., 2013. What drives the seasonality of photosynthesis across the Amazon basin? A cross-site analysis of eddy flux tower measurements from the Brasil flux network. *Agric. For. Meteorol.* <https://doi.org/10.1016/j.agrformet.2013.04.031>.
- Rice, W.R., 1989. Analyzing tables of statistical tests. *Evolution* (N. Y.) 43, 223–225. <https://doi.org/10.2307/2409177>.
- Richardson, A.D., Braswell, B.H., Hollinger, D.Y., Jenkins, J.P., Ollinger, S.V., 2009. Near-surface remote sensing of spatial and temporal variation in canopy phenology. *Ecol. Appl.* 19, 1417–1428. <https://doi.org/10.1890/08-2022.1>.
- Roderick, M.L., Farquhar, G.D., 2002. The cause of decreased Pan evaporation over the past 50 years. *Science* 298 (80), 1410–1411.
- Roupsard, O., Bonnefond, J.-M., Irvine, M., Berbigier, P., Nouvellon, Y., Dautat, J., Taga, S., Hamel, O., Jourdan, C., Saint-André, L., Miallet-Serra, I., Labouisse, J.-P., Epron, D., Joffre, R., Braconnier, S., Rouzière, A., Navarro, M., Bouillet, J.-P., 2006. Partitioning energy and evapo-transpiration above and below a tropical palm canopy. *Agric. For. Meteorol.* 139, 252–268. <https://doi.org/10.1016/j.agrformet.2006.07.006>.
- Saleska, S.R., Miller, S.D., Matross, D.M., Goulden, M., Wofsy, S., da Rocha, H.R., de Camargo, P.B., Crill, P., Daube, B.C., de Freitas, H.C., Hutyrá, L., Keller, M., Kirchhoff, V., Menton, M., Munger, J.W., Pyle, E.H., Rice, A.H., Silva, H., 2003. Carbon in Amazon forests: unexpected seasonal fluxes and disturbance-induced losses. *Science* 302 (80), 1554–1557.
- Saleska, S.R., Didan, K., Huete, A.R., Da Rocha, H.R., 2007. Amazon forests green-up during 2005 drought. *Science* 318 (80), 612.
- Saleska, S., Da Rocha, H., Kruijt, B., Nobre, A., 2009. Ecosystem carbon fluxes and Amazonian forest metabolism. *Amazonia Glob. Change* 389–407. <https://doi.org/10.1029/2008GM000739>.
- Saleska, S.R., Wu, J., Guan, K., Araujo, A.C., Huete, A., Nobre, A.D., Restrepo-Coupe, N., 2016. Dry-season greening of Amazon forests. *Nature* 531, E4–E5.
- Salinas, N., Malhi, Y., Meir, P., Silman, M., Roman Cuesta, R., Huaman, J., Salinas, D., Huaman, V., Gibaja, A., Mamani, M., Farfan, F., 2011. The sensitivity of tropical leaf litter decomposition to temperature: results from a large-scale leaf translocation experiment along an elevation gradient in Peruvian forests. *New Phytol.* 189, 967–977. <https://doi.org/10.1111/j.1469-8137.2010.03521.x>.
- Santana, R.A., Dias-Júnior, C.Q., da Silva, J.T., Fuentes, J.D., do Vale, R.S., Alves, E.G., dos Santos, R.M.N., Manzi, A.O., 2018. Air turbulence characteristics at multiple sites in and above the Amazon rainforest canopy. *Agric. For. Meteorol.* 260–261, 41–54. <https://doi.org/10.1016/j.agrformet.2018.05.027>.
- Santos, D.M., Acevedo, O.C., Chamecki, M., Fuentes, J.D., Gerken, T., Stoy, P.C., 2016. Temporal scales of the nocturnal flow within and above a forest canopy in Amazonia. *Boundary-Layer Meteorol.* 1–26. <https://doi.org/10.1007/s10546-016-0158-5>.
- Siddiq, Z., Chen, Y.-J., Zhang, Y.-J., Zhang, J.-L., Cao, K.-F., 2017. More sensitive response of crown conductance to VPD and larger water consumption in tropical evergreen than in deciduous broadleaf timber trees. *Agric. For. Meteorol.* 247, 399–407. <https://doi.org/10.1016/j.agrformet.2017.08.028>.
- Sulman, B.N., Roman, D.T., Yi, K., Wang, L., Phillips, R.P., Novick, K.A., 2016. High atmospheric demand for water can limit forest carbon uptake and transpiration as severely as dry soil. *Geophys. Res. Lett.* 43, 9686–9695. <https://doi.org/10.1002/2016GL069416>.
- Swann, A.L.S., Hoffman, F.M., Koven, C.D., Randerson, J.T., 2016. Plant responses to increasing CO<sub>2</sub> reduce estimates of climate impacts on drought severity. *Proc. Natl. Acad. Sci. U. S. A.* 113, 10019–10024. <https://doi.org/10.1073/pnas.1604581113>.
- Taylor, K.E., Stouffer, R.J., Meehl, G.A., 2012. An overview of CMIP5 and the experiment design. *Bull. Am. Meteorol. Soc.* <https://doi.org/10.1175/BAMS-D-11-00094.1>.
- Taylor, P.G., Cleveland, C.C., Wieder, W.R., Sullivan, B.W., Dougherty, C.E., Dobrowski, S.Z., Townsend, A.R., 2017. Temperature and rainfall interact to control carbon cycling in tropical forests. *Ecol. Lett.* 20, 779–788. <https://doi.org/10.1111/ele.12765>.
- Thomas, C.K., Martin, J.G., Law, B.E., Davis, K., 2013. Toward biologically meaningful net carbon exchange estimates for tall, dense canopies: multi-level eddy covariance observations and canopy coupling regimes in a mature Douglas-fir forest in Oregon. *Agric. For. Meteorol.* 173, 14–27. <https://doi.org/10.1016/j.agrformet.2013.01.001>.
- Tóta, J., Fitzjarrald, D.R., da Silva Dias, M.A.F., 2012. Amazon rainforest exchange of carbon and subcanopy air flow: Manaus LBA Site—a complex terrain condition. *Transfus. Apher. Sci.* <https://doi.org/10.1100/2012/165067>. 165067.
- Tyukavina, A., Baccini, A., Hansen, M.C., Potapov, P.V., Stehman, S.V., Houghton, R.A., Krylov, A.M., Turubanova, S., Goetz, S.J., 2015. Aboveground carbon loss in natural and managed tropical forests from 2000 to 2012. *Environ. Res. Lett.* 10, 74002.
- van Marle, M.J.E., Field, R.D., van der Werf, G.R., Estrada de Wagt, I.A., Houghton, R.A., Rizzo, L.V., Artaxo, P., Tsigaridis, K., 2017. Fire and deforestation dynamics in Amazonia (1973–2014). *Glob. Biogeochem. Cycles* 31, 24–38. <https://doi.org/10.1002/2016GB005445>.
- Wieder, W.R., Cleveland, C.C., Townsend, A.R., 2009. Controls over leaf litter decomposition in wet tropical forests. *Ecology* 90, 3333–3341. <https://doi.org/10.1890/08-2294.1>.
- Wolf, S., Eugster, W., Majorek, S., Buchmann, N., 2011a. Afforestation of tropical pasture only marginally affects ecosystem-scale evapotranspiration. *Ecosystems* 14, 1264–1275.
- Wolf, S., Eugster, W., Potvin, C., Buchmann, N., 2011b. Strong seasonal variations in net ecosystem CO<sub>2</sub> exchange of a tropical pasture and afforestation in Panama. *Agric. For. Meteorol.* 151, 1139–1151.
- Wolf, S., Eugster, W., Potvin, C., Turner, B.L., Buchmann, N., 2011c. Carbon sequestration potential of tropical pasture compared with afforestation in Panama. *Glob. Change Biol.* 17, 2763–2780. <https://doi.org/10.1111/j.1365-2486.2011.02460.x>.
- Wood, A.W., Leung, L.R., Sridhar, V., Lettenmaier, D.P., 2004. Hydrologic implications of dynamical and statistical approaches to downscaling climate model outputs. *Clim. Change* 62, 189–216. <https://doi.org/10.1023/B:CLIM.0000013685.99609.9e>.
- Wu, J., Guan, K., Hayek, M., Restrepo-Coupe, N., Wiedemann, K.T., Xu, X., Wehr, R., Christoffersen, B.O., Miao, G., da Silva, R., de Araujo, A.C., Oliviera, R.C., Camargo, P.B., Monson, R.K., Huete, A.R., Saleska, S.R., 2017. Partitioning controls on Amazon forest photosynthesis between environmental and biotic factors at hourly to inter-annual timescales. *Glob. Change Biol.* 23, 1240–1257. <https://doi.org/10.1111/gcb.13509>.
- Xiao, J., Liu, S., Stoy, P.C., 2016. Preface: impacts of extreme climate events and disturbances on carbon dynamics. *Biogeosciences* 13, 3665–3675. <https://doi.org/10.5194/bg-13-3665-2016>.